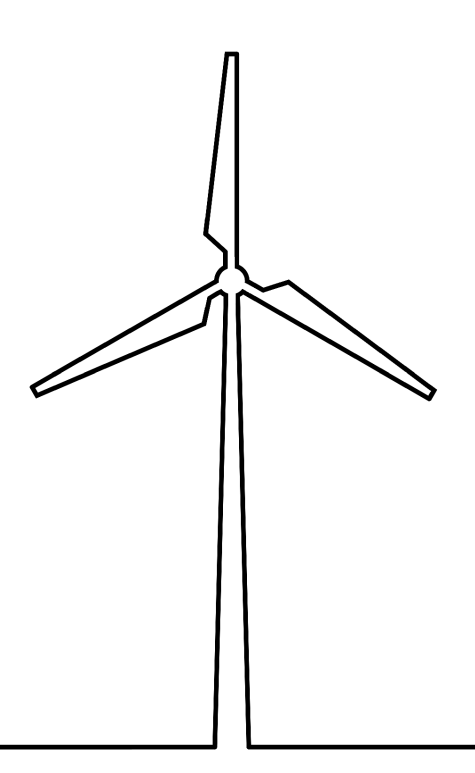
Optimization of a wind turbine blade-root connection

Athul Narayana Rao



Faculty of Aerospace Engineering \cdot Delft University of Technology





Optimization of a wind turbine blade-root connection

MASTER OF SCIENCE THESIS

For obtaining the degree of Master of Science in Aerospace Engineering at Delft University of Technology

Athul Narayana Rao

14/9/2017

The work in this thesis was supported by Suzlon Energy Limited - Netherlands. Their cooperation is gratefully acknowledged.





DELFT UNIVERSITY OF TECHNOLOGY FACULTY OF AEROSPACE ENGINEERING DEPARTMENT OF AEROSPACE STRUCTURES AND MATERIALS

GRADUATION COMMITTEE

	Dated: <u>14/9/2017</u>
Chair holder:	Dr.ir. Roeland de Breuker
Committee members:	Dr.ir. Sonell Shroff
	ir. Valter Luis Bellotto
	Dr.ir. Calvin Rans

Abstract

For several years T-bolts have been a popular choice for joints in the field of wind energy, specifically for connecting the blade roots to the hub of the wind turbine. Their use is mandated by the geometry of the joint and they perform very well under pure axial loading. However recent analyses have shown significant bending stresses in the T-bolts preventing their use to their full capacity. These bending stresses are unavoidable due to the presence of a slew bearing between the blade root and the hub. The bending stresses generated while loading the blade root, causes the blade root-bearing joint to gradually open, causing excessive loading of the T-bolt above a certain load.

It is hypothesized that modifying the blade root design to reduce the effects of local bending can open up the possibility of reducing its mass and cost. To test this hypothesis, the blade root is initially studied and the stress ratio is identified as an appropriate joint performance parameter. The performance of the joint is boosted by increasing the pretension of the bolt. After an initial phase of over designing the joint to reduce the constraint stresses, the joint optimization is carried out using the Sequential Quadratic Programming algorithm. The optimization culminates with the mass reducing by roughly 110Kg and the material cost reducing by approximately 13% per blade root. The number of bolts reduces from 88 to 52. Thus, a simpler design is achieved, that promises simpler and cheaper manufacturability, higher reliability and lesser sites for crack nucleation in the laminates.

The current design strategy at Suzlon is to employ a greater number of T-bolts with thinner shanks. Curiosity in the field of cost optimization that initiated from within Suzlon has proved that there exists a different design strategy that holds great promise for delivering structurally equivalent if not better designs with improved cost, mass and reliability.

Table of Contents

	Abb	reviations	xvii
	List	of Symbols	xix
	Pref	ace	xxiii
	Ack	nowledgments	xxv
1	Intro	oduction	1
	1.1	The blade root connection	1
	1.2	Problem statement by Suzlon and research objective	3
	1.3	Reader's guide	4
2	Lite	rature survey and theoretical foundations	5
	2.1	The T-bolt connection	5
	2.2	Fatigue in bolted connections	5
	2.3	Optimization of bolted connection	6
	2.4	Blade root connection - Popular designs	7
	2.5	Forces and stresses at blade root connection	7
	2.6	Composites general information	8
	2.7	General composite failure modes	9
	2.8	Bolted joints	10
		2.8.1 Shear loaded bolted joints	11
		2.8.2 Tension loaded bolted joint	12
	2.9	T-bolt joint	13
		2.9.1 T-bolt properties and parameters	13
		2.9.2 Stresses in a T-bolt	14
		2.9.3 Maximum expected load	15

Table of Contents

		2.9.4	Fatigue analysis	15
	2.10	Optimi	zation problems	16
		2.10.1	Basic framework	17
				17
				18
		2.10.4	Algorithms	18
		2.10.5	General performance of the algorithms	19
	2.11	Researc	ch question	20
	2.12	Conclus	sion - Literature survey	21
		2.12.1	Optimization - outcome & expectation	21
		2.12.2	Design guidelines	21
3	Finit	e elem	ent model and optimization framework	23
•	3.1			23
	3.2			$\frac{25}{24}$
	J.2	3.2.1		$\frac{24}{24}$
		3.2.2		24
		3.2.3		26
		3.2.4	Boundary conditions	27
		3.2.5	Element types in reduced model	28
	3.3	Materia	al properties	29
	3.4	Optimi:	zation framework	29
	3.5	Constra	aint functions	32
		3.5.1	Bearing failure	32
		3.5.2		33
		3.5.3		33
		3.5.4		34
	2.6	3.5.5	S	34
	3.6	Optimi	zation algorithms	35
4	Opti	mizatio	on :	37
	4.1	Genera	l ideology behind the optimization procedure	37
		4.1.1	Optimization and convergence	37
		4.1.2	Convergence	38
		4.1.3	Ideology	38
	4.2	Stress i	ratio and joint behavior	39
	4.3	Parame	eter identification	40
		4.3.1	Cost function parameters	40
		4.3.2	Constraint parameters	41
	4.4	Initial o	over design of the blade root and its implications	42
	4.5		- · · · · · · · · · · · · · · · · · · ·	43
	4.6			45
	4.7			46
		4.7.1	•	47
		4.7.2		48

T 11 C C	
Table of Contents	Y1

5	Resi	ults and	d conclusions	51
	5.1	Design	recommendations	51
		5.1.1	Prestress in the bolts	51
		5.1.2	T-bolt and blade root dimensions	52
	5.2	Implica	ations of the design recommendation	52
		5.2.1	Cost implications	53
		5.2.2	Manufacturing implications	55
		5.2.3	Fatigue life and maintenance implication	55
		5.2.4	Effects on bearings	56
	5.3	Conclu	usions	56
Re	ferer	ices		60
	Refe	erences		61
Α	Bou	ndary o	condition conversion	63
	A.1	Bound	ary condition in Half model	63
	A.2	Bound	ary condition in Section model	64
В	Blac	le root	dimensions	67
	B.1	Dimen	sions of the blade root	67
	B.2	Model	simplification	68

xii Table of Contents

List of Figures

1.1	Blade root-hub bearing and pitch control gear system	2
1.2	Hub slew bearing	2
2.1	Bushing connection	7
2.2	T-bolt connection	7
2.3	Stacking sequence	3
2.4	Ply directions)
2.5	Stress planes)
2.6	Bolted joints failure modes)
2.7	Bolt/rivet failure modes	L
2.8	T-Bolt with limited access	L
2.9	Bolt loaded in tension	2
2.10	Perpendicularity of members in T-bolt connection	2
2.11	Bolted joint working diagram	3
2.12	Axial stresses in bolt	1
2.13	Sample SN curve	3
3.1	Illustration of the features of blade root model	5
3.2	Method of introduction of load into the reduced model	3
3.3	Boundary condition at the bearing	7
3.4	Planes of symmetry extracted for clarity	7
3.5	Illustration of elements used in the blade root model	3
3.6	Flow chart of the cost function)
3.7	Stress planes in the laminate	2
4.1	Stress ratio increase in reference design during joint opening)
4.2	Stress ratio after increasing pretension in the bolt)

xiv List of Figures

4.3	Prestress - 540MPa	40
4.4	Prestress - 640MPa	40
4.5	Blade root optimization parameters	41
4.6	Convergence of optimizer	46
4.7	SN curve for optimized design	48
4.8	Stress ratio comparison - Half model vs Sectional model	49
5.1	Cost-mass relation	53
5.2	Influence of material rates	53
5.3	Region of modification	54
A.1	Illustration of plane of symmetry in Half model	63
A.2	Illustration of plane of symmetry in Sectional model	64
A.3	Illustration of laminate stresses	65
B.1	Dimensions of Reference design	68
B 2	Dimensions of Ontimized design	68

List of Tables

2.1	Design limits of constraint stresses	17
2.2	Algorithm performance study	19
3.1	Material properties of Steel and GFRP	29
4.1	Initial constraint stress values and their limits	42
4.2	Mass and cost comparison (Reference vs over design)	43
4.3	Constraint stresses after initial over design	43
4.4	Optimization parameters and their boundaries	44
4.5	Dimensions and properties of Reference design	44
4.6	Dimensions and properties of Optimized design 1	44
4.7	Constraint stresses in optimized design	45
4.8	Bhd and Br at the three stages of optimization	45
4.9	Fatigue analysis results	48
5.1	Reference design - cost and mass	53

xvi List of Tables

Abbreviations

GFRP Glass Fiber Reinforced Plastic

SBT Suzlon Blade Technology

FEM Finite Element Method

FRP Fiber Reinforced Plastic

RHS Right Hand Side

GUI Graphical User Interface

CG Conjugate Gradient

COBYLA Constrained Optimization BY Linear Approximation

SLSQP Sequential Large Scale Quadratic Programming

SQP Sequential Quadratic Programming

DE Differential Evolution

APDL Ansys Parametric Design Language

PIP Installs Packages

DNV Det Norske Veritas

GL Germanischer Lloyd

DaEq Damage Equivalent

xviii Abbreviations

List of Symbols

α	Linear coefficient of thermal expansion	$[K^{-1}]$
μ_{xy}	XY Poisson's ratio	[-]
μ_{xz}	XZ Poisson's ratio	[-]
μ_{yz}	YZ Poisson's ratio	[-]
Φ	Stress ratio of the joint	[-]
$\sigma_{ m axial}$	Total axial stress due to external loading	[Pa]
$\sigma_{ m bending}$	Total bending stress due to external loading	[Pa]
$\sigma_{ m pl}$	Preload stress	[Pa]
σ_{bolt}	Stress due to default temperature application	[Pa]
σ_{Mean}	Mean stress due to loading	[Pa]
$\sigma_{prestress}$	Stress due to preload	[Pa]
σ_{Range}	Range of the stress due to loading	[Pa]
$\sigma_{ m ax_total}$	Maximum tensile stress in the bolt	[Pa]
$\sigma_{ m ut_comp}$	Ultimate compressive strength of laminate	[Pa]
$\sigma_{ m ut_shear}$	Ultimate shear strength of laminate	[Pa]
$\sigma_{ m ut_tens}$	Ultimate tensile strength of laminate	[Pa]
$\sigma_{ m yeild}$	Yield stress of the bolt	[Pa]
au	Shear stress due to torquing of bolt	[Pa]
$ heta_{ m bolt}$	Angular position of bolt in blade root	[Rad]
$\theta_{ m sector}$	Internal angle of model sector	[Rad]
A_{bearing}	Bearing area of bolted joint	$[m^2]$
$A_{\text{netsection}}$	Net-section area of bolted joint	$[m^2]$
$A_{\rm shearout}$	Shear area of bolted joint	$[m^2]$
Bd	Bolt shank diameter	[m]
Bhd	Barrel head diameter	[m]
E_x	Young's modulus in X direction	[Pa]
E_y	Young's modulus in Y direction	[Pa]
E_z	Young's modulus in Z direction	[Pa]

xx List of Symbols

F_{ext} Force equivalent of external bending moment $[N]$ $g_t(x)$ Inequality constraints function $[-]$ G_{xy} Shear modulus along XY plane $[Pa]$ G_{yz} Shear modulus in YZ plane $[Pa]$ $h_t(x)$ Inequality constraints function $[-]$ k_s SN curve knock down factor $[-]$ K_b Effective stiffness of the bolt $[N/m]$ K_m Effective stiffness of the blade root (Parameter) $[m]$ $L1$ Length of the thick part of the blade root (Parameter) $[m]$ $L2$ Length of the transition part of the blade root (Parameter) $[m]$ M_g Moment required to produce the pretension $[Nm]$ M_{max} External bending moment on blade root $[Nm]$ M_{max} Maximum bending moment in a loading sequence $[Nm]$ M_{max} Maximum bending moment in a loading sequence $[Nm]$ M_{max} Manumber of Dolts in the blade root (Parameter) $[-]$ N_b Number of T-bolts in the blade root (Parameter) $[-]$ N_b	f(x)	Cost or fitness function	[-]
$ \begin{array}{cccccccccccccccccccccccccccccccccccc$	F_{ext}	Force equivalent of external bending moment	[N]
$ \begin{array}{c} G_{xz} & \text{Shear modulus in the XZ plane} & [Pa] \\ G_{yz} & \text{Shear modulus in YZ plane} & [Pa] \\ h_i(x) & \text{Inequality constraints function} & [-] \\ k_s & \text{SN curve knock down factor} & [-] \\ K_{\text{b}} & \text{Effective stiffness of the bolt} & [N/m] \\ K_{\text{m}} & \text{Effective stiffness of the flanges} & [N/m] \\ L1 & \text{Length of the thick part of the blade root (Parameter)} & [m] \\ L2 & \text{Length of the transition part of the blade root (Parameter)} & [m] \\ M_g & \text{Moment required to produce the pretension} & [Nm] \\ M_{mext} & \text{External bending moment on blade root} & [Nm] \\ M_{Mox} & \text{Maximum bending moment in a loading sequence} & [Nm] \\ M_{Mox} & \text{Maximum bending moment in a loading sequence} & [Nm] \\ M_{Min} & \text{Bending moment range in a loading sequence} & [Nm] \\ M_{Min} & \text{Bending moment range in a loading sequence} & [Nm] \\ M_{bolts} & \text{Number of T-bolts in the blade root} & [-] \\ P & \text{External load on the joint} & [N] \\ P_b & \text{Load absorbed by bolt} & [N] \\ P_m & \text{Load absorbed by flanges} & [N] \\ P_{Max} & \text{Max equivalent load in loading sequence} & [N] \\ P_{Min} & \text{Min equivalent load in loading sequence} & [N] \\ R_i & \text{Blade root inner radius (Parameter)} & [m] \\ R_i & \text{Blade root inner radius (Parameter)} & [m] \\ T_{default} & \text{Default temperature} & [K] \\ W_P & \text{Moment of resistance} & [m^3] \\ x & \text{Parameter set} & [-] \\ x^{L} & \text{Lower bounds} & [-] \\ - x^{U} & \text{Upper bounds} & [-] \\ \sigma_{\text{ext.max}} & \text{Maximum stress due to external loading} & [Pa] \\ \sigma_{\text{bolt max}} & \text{Bolt stress at extreme loading} & [Pa] \\ F_{pl} & \text{Bolt preload force} & [N] \\ K_{joint} & \text{Stiffness of the joint} & [m] \\ F_{bolt} & \text{Temperature to be applied for required prestress} & [K] \\ E_G & \text{Static friction coefficient} & [-] \\ A_b & \text{Effective area of the bolt} & [m^2] \\ \end{array}$	$g_i(x)$	Inequality constraints function	[-]
$ \begin{array}{c} G_{xz} & \text{Shear modulus in the XZ plane} & [Pa] \\ G_{yz} & \text{Shear modulus in YZ plane} & [Pa] \\ h_i(x) & \text{Inequality constraints function} & [-] \\ k_s & \text{SN curve knock down factor} & [-] \\ K_{\text{b}} & \text{Effective stiffness of the bolt} & [N/m] \\ K_{\text{m}} & \text{Effective stiffness of the flanges} & [N/m] \\ L1 & \text{Length of the thick part of the blade root (Parameter)} & [m] \\ L2 & \text{Length of the transition part of the blade root (Parameter)} & [m] \\ M_g & \text{Moment required to produce the pretension} & [Nm] \\ M_{mext} & \text{External bending moment on blade root} & [Nm] \\ M_{Mox} & \text{Maximum bending moment in a loading sequence} & [Nm] \\ M_{Mox} & \text{Maximum bending moment in a loading sequence} & [Nm] \\ M_{Min} & \text{Bending moment range in a loading sequence} & [Nm] \\ M_{Min} & \text{Bending moment range in a loading sequence} & [Nm] \\ M_{bolts} & \text{Number of T-bolts in the blade root} & [-] \\ P & \text{External load on the joint} & [N] \\ P_b & \text{Load absorbed by bolt} & [N] \\ P_m & \text{Load absorbed by flanges} & [N] \\ P_{Max} & \text{Max equivalent load in loading sequence} & [N] \\ P_{Min} & \text{Min equivalent load in loading sequence} & [N] \\ R_i & \text{Blade root inner radius (Parameter)} & [m] \\ R_i & \text{Blade root inner radius (Parameter)} & [m] \\ T_{default} & \text{Default temperature} & [K] \\ W_P & \text{Moment of resistance} & [m^3] \\ x & \text{Parameter set} & [-] \\ x^{L} & \text{Lower bounds} & [-] \\ - x^{U} & \text{Upper bounds} & [-] \\ \sigma_{\text{ext.max}} & \text{Maximum stress due to external loading} & [Pa] \\ \sigma_{\text{bolt max}} & \text{Bolt stress at extreme loading} & [Pa] \\ F_{pl} & \text{Bolt preload force} & [N] \\ K_{joint} & \text{Stiffness of the joint} & [m] \\ F_{bolt} & \text{Temperature to be applied for required prestress} & [K] \\ E_G & \text{Static friction coefficient} & [-] \\ A_b & \text{Effective area of the bolt} & [m^2] \\ \end{array}$	G_{xy}	Shear modulus along XY plane.	[Pa]
$\begin{array}{cccccccccccccccccccccccccccccccccccc$		Shear modulus in the XZ plane	[Pa]
$\begin{array}{cccccccccccccccccccccccccccccccccccc$	G_{yz}	Shear modulus in YZ plane	[Pa]
$ \begin{array}{c} K_{\rm b} \\ K_{\rm m} \\ Effective stiffness of the bolt \\ K_{\rm m} \\ Effective stiffness of the flanges \\ [N/m] \\ K_{\rm m} \\ Effective stiffness of the flanges \\ [N/m] \\ L1 \\ Length of the thick part of the blade root (Parameter) \\ [m] \\ L2 \\ Length of the transition part of the blade root (Parameter) \\ [m] \\ M_g \\ Moment required to produce the pretension \\ [Nm] \\ M_{ext} \\ External bending moment on blade root \\ [Nm] \\ M_{Max} \\ Maximum bending moment in a loading sequence \\ [Nm] \\ M_{Man} \\ Mean bending moment in a loading sequence \\ [Nm] \\ M_{Min} \\ Bending moment range in a loading sequence \\ [Nm] \\ M_{mange} \\ Bending moment range in a loading sequence \\ [Nm] \\ N_{bolts} \\ Number of T-bolts in the blade root \\ [-] \\ Nb \\ Number of bolts in the blade root (Parameter) \\ [-] \\ P \\ External load on the joint \\ P_{\rm m} \\ Load absorbed by bolt \\ P_{\rm m} \\ Load absorbed by flanges \\ [N] \\ P_{max} \\ Max equivalent load in loading sequence \\ [N] \\ P_{max} \\ Max equivalent load in loading sequence \\ [N] \\ P_{min} \\ Min equivalent load in loading sequence \\ [N] \\ R_{io} \\ Blade root inner radius (Parameter) \\ [m] \\ T_{default} \\ Default temperature \\ [m] \\ W_{P} \\ Moment of resistance \\ [m] \\ T_{default} \\ Upper bounds \\ [-] \\ \sigma_{ext_max} \\ Maximum stress due to external loading \\ [-] \\ \sigma_{ext_max} \\ Maximum stress due to external loading \\ [-] \\ \sigma_{bolt max} \\ Bolt stress at extreme loading \\ [-] \\ P_{pl} \\ Bolt preload force \\ [N] \\ K_{joint} \\ Stiffness of the joint \\ [-] \\ T_{bolt} \\ Temperature to be applied for required prestress \\ [K] \\ M_{G} \\ Static friction coefficient \\ [-] \\ -] \\ A_{b} \\ Effective area of the bolt \\ [m] \\ [m] \\ [m] \\ T_{out} \\ [m] \\ T_{out} \\$		Inequality constraints function	[-]
$ \begin{array}{c} K_{\rm m} & {\rm Effective~stiffness~of~the~flanges} & [N/m] \\ L1 & {\rm Length~of~the~thick~part~of~the~blade~root~(Parameter)} & [m] \\ L2 & {\rm Length~of~the~transition~part~of~the~blade~root~(Parameter)} & [m] \\ M_g & {\rm Moment~required~to~produce~the~pretension} & [Nm] \\ M_{ext} & {\rm External~bending~moment~on~blade~root} & [Nm] \\ M_{Max} & {\rm Maximum~bending~moment~in~a~loading~sequence} & [Nm] \\ M_{Mam} & {\rm Mean~bending~moment~in~a~loading~sequence} & [Nm] \\ M_{Mam} & {\rm Bending~moment~range~in~a~loading~sequence} & [Nm] \\ M_{Range} & {\rm Bending~moment~range~in~a~loading~sequence} & [Nm] \\ M_{Range} & {\rm Bending~moment~range~in~a~loading~sequence} & [Nm] \\ N_{bolts} & {\rm Number~of~T-bolts~in~the~blade~root} & [-] \\ Nb & {\rm Number~of~bolts~in~the~blade~root} & [-] \\ Nb & {\rm Number~of~bolts~in~the~blade~root} & [N] \\ P_{\rm m} & {\rm Load~absorbed~by~bolt} & [N] \\ P_{\rm m} & {\rm Load~absorbed~by~bolt} & [N] \\ P_{m} & {\rm Load~absorbed~by~flanges} & [N] \\ P_{max} & {\rm Max~equivalent~load~in~loading~sequence} & [N] \\ N_{m} & {\rm Min~equivalent~load~in~loading~sequence} & [N] \\ N_{m} & {\rm Min~equivalent~load~in~loading~sequence} & [m] \\ R_{i} & {\rm Blade~root~inmer~radius~(Parameter)} & [m] \\ T_{default} & {\rm Default~temperature} & [K] \\ W_{P} & {\rm Moment~of~resistance} & [m] \\ x & {\rm Parameter~set} & [-] \\ x^{\rm U} & {\rm Upper~bounds} & [-] \\ \sigma_{\rm ext_max} & {\rm Maximum~stress~due~to~external~loading} & [Pa] \\ \sigma_{\rm bolt~max} & {\rm Bolt~stress~at~exterme~loading} & [Pa] \\ F_{\rm pl} & {\rm Stiffness~of~the~joint}} & [\frac{m}{n}] \\ T_{bolt} & {\rm Temperature~to~be~applied~for~required~prestress} & [K] \\ H_{G} & {\rm Static~friction~coefficient} & [-] \\ A_{b} & {\rm Effective~area~of~the~bolt} & [m] \\ \end{array}$	k_s	SN curve knock down factor	[-]
L1 Length of the thick part of the blade root (Parameter) $[m]$ L2 Length of the transition part of the blade root (Parameter) $[m]$ M_g Moment required to produce the pretension $[Nm]$ M_{ext} External bending moment on blade root $[Nm]$ M_{Max} Maximum bending moment in a loading sequence $[Nm]$ M_{Mean} Mean bending moment range in a loading sequence $[Nm]$ M_{Min} Bending moment range in a loading sequence $[Nm]$ M_{Range} Bending moment range in a loading sequence $[Nm]$ N_{bolts} Number of T-bolts in the blade root $[-]$ N_b Number of D-bolts in the blade root (Parameter) $[-]$ N_b Number of bolts in the blade root (Parameter) $[-]$ P_b Load absorbed by bolt $[N]$ P_b Load absorbed by flanges $[N]$ P_{max} Max equivalent load in loading sequence $[N]$ P_{Min} Min equivalent load in loading sequence $[N]$ R_{total} Average blade root radius $[m]$ R_{total} $[n]$ $[n]$ R_{total}	$K_{ m b}$	Effective stiffness of the bolt	[N/m]
$L2$ Length of the transition part of the blade root (Parameter) $[m]$ M_g Moment required to produce the pretension $[Nm]$ M_{ext} External bending moment on blade root $[Nm]$ M_{Max} Maximum bending moment in a loading sequence $[Nm]$ M_{Mean} Mean bending moment range in a loading sequence $[Nm]$ M_{Min} Bending moment range in a loading sequence $[Nm]$ M_{Range} Bending moment range in a loading sequence $[Nm]$ N_{botts} Number of T-botts in the blade root $[-]$ N_{botts} Number of Doubts in the blade root (Parameter) $[-]$ N_{botts} Number of botts in the blade root (Parameter) $[-]$ N_{botts} Number of botts in the blade root (Parameter) $[-]$ P_{b} Load absorbed by bott $[N]$ P_{m} Load absorbed by flanges $[N]$ P_{m} Load absorbed by flanges $[N]$ P_{max} Max equivalent load in loading sequence $[N]$ P_{max} Max equivalent load in loading sequence $[N]$ R_{io} Average blade root radius $[n]$	$K_{ m m}$	Effective stiffness of the flanges	[N/m]
$ \begin{array}{c ccccccccccccccccccccccccccccccccccc$	L1	Length of the thick part of the blade root (Parameter)	[m]
M_{ext} External bending moment on blade root $[Nm]$ M_{Max} Maximum bending moment in a loading sequence $[Nm]$ M_{Mean} Mean bending moment in a loading sequence $[Nm]$ M_{Min} Bending moment range in a loading sequence $[Nm]$ M_{Range} Bending moment range in a loading sequence $[Nm]$ N_{bolts} Number of T-bolts in the blade root $[-]$ N_b Number of bolts in the blade root (Parameter) $[-]$ P External load on the joint $[N]$ P_b Load absorbed by bolt $[N]$ P_m Load absorbed by flanges $[N]$ P_{max} Max equivalent load in loading sequence $[N]$ P_{max} Max equivalent load in loading sequence $[N]$ P_{min} Min equivalent load in loading sequence $[N]$ R_{root} Average blade root radius $[m]$ R_{root} Average blade root radius (Parameter) $[m]$ R_{i} Blade root inner radius (Parameter) $[m]$ R_{i} Default temperature $[K]$ W_{P} Moment of resistance <t< td=""><td>L2</td><td>Length of the transition part of the blade root (Parameter)</td><td>[m]</td></t<>	L2	Length of the transition part of the blade root (Parameter)	[m]
M_{Max} Maximum bending moment in a loading sequence $[Nm]$ M_{Mean} Mean bending moment in a loading sequence $[Nm]$ M_{Min} Bending moment range in a loading sequence $[Nm]$ M_{Range} Bending moment range in a loading sequence $[Nm]$ N_{bolts} Number of T-bolts in the blade root $[-]$ N_b Number of bolts in the blade root $[-]$ P External load on the joint $[N]$ P_b Load absorbed by bolt $[N]$ P_m Load absorbed by flanges $[N]$ P_m Load absorbed by flanges $[N]$ P_{max} Max equivalent load in loading sequence $[N]$ P_{max} Max equivalent load in loading sequence $[N]$ P_{max} Average blade root radius $[m]$ R_{toot} Average blade root radius $[m]$ R_t Blade root inner radius (Parameter) $[m]$ R_t Blade root inner radius (Parameter) $[m]$ R_t Bofault temperature $[K]$ W_P Moment of resistance $[m]$ x^t	M_g	Moment required to produce the pretension	[Nm]
M_{Mean} Mean bending moment in a loading sequence $[Nm]$ M_{Min} Bending moment range in a loading sequence $[Nm]$ M_{Range} Bending moment range in a loading sequence $[Nm]$ N_{bolts} Number of T-bolts in the blade root $[-]$ N_b Number of bolts in the blade root (Parameter) $[-]$ P External load on the joint $[N]$ P_b Load absorbed by bolt $[N]$ P_m Load absorbed by flanges $[N]$ P_{max} Max equivalent load in loading sequence $[N]$ P_{Max} Max equivalent load in loading sequence $[N]$ P_{min} Min equivalent load in loading sequence $[N]$ P_{min} Min equivalent load in loading sequence $[N]$ P_{min} Average blade root radius $[m]$ R_{min} $[m]$ $[m]$ <t< td=""><td>M_{ext}</td><td>External bending moment on blade root</td><td>[Nm]</td></t<>	M_{ext}	External bending moment on blade root	[Nm]
M_{Min} Bending moment range in a loading sequence $[Nm]$ M_{Range} Bending moment range in a loading sequence $[Nm]$ N_{bolts} Number of T-bolts in the blade root $[-]$ Nb Number of bolts in the blade root (Parameter) $[-]$ P External load on the joint $[N]$ P Load absorbed by bolt $[N]$ P_{m} Load absorbed by flanges $[N]$ P_{max} Max equivalent load in loading sequence $[N]$ P_{Min} Min equivalent load in loading sequence $[N]$ R_{root} Average blade root radius $[m]$ R_{i} Blade root inner radius (Parameter) $[m]$ $T_{default}$ Default temperature $[K]$ W_P Moment of resistance $[m]$ x Parameter set $[-]$ x^L Lower bounds $[-]$ x^U Upper bounds $[-]$ σ_{ext_max} Maximum stress due to external loading $[Pa]$ $\sigma_{bolt\ max}$ Bolt stress at extreme loading $[Pa]$ F_{pl} Bolt preload force $[N]$ K_{joint} Stiffness of the joint $[\frac{N}{m}]$ T_{bolt} Temperature to be applied for required prestress $[K]$ μ_G Static friction coefficient $[-]$ A_b Effective area of the bolt $[m]$	M_{Max}	Maximum bending moment in a loading sequence	[Nm]
M_{Range} Bending moment range in a loading sequence $[Nm]$ N_{bolts} Number of T-bolts in the blade root $[-]$ Nb Number of bolts in the blade root (Parameter) $[-]$ P External load on the joint $[N]$ P Load absorbed by bolt $[N]$ P_{m} Load absorbed by flanges $[N]$ P_{max} Max equivalent load in loading sequence $[N]$ P_{Min} Min equivalent load in loading sequence $[N]$ R_{root} Average blade root radius $[m]$ R_{i} Blade root inner radius (Parameter) $[m]$ $T_{default}$ Default temperature $[K]$ W_P Moment of resistance $[m]^3$ x Parameter set $[-]$ x^{L} Lower bounds $[-]$ x^{U} Upper bounds $[-]$ σ_{ext_max} Maximum stress due to external loading $[Pa]$ $\sigma_{\text{bolt max}}$ Bolt stress at extreme loading $[Pa]$ F_{pl} Bolt preload force $[N]$ K_{joint} Stiffness of the joint $[N]$ T_{bolt} Temperature to be applied for required prestress $[K]$ μ_G Static friction coefficient $[-]$ A_b Effective area of the bolt $[m^2]$	M_{Mean}	Mean bending moment in a loading sequence	[Nm]
N_{bolts} Number of T-bolts in the blade root (Parameter)[-] Nb Number of bolts in the blade root (Parameter)[-] P External load on the joint[N] P_{b} Load absorbed by bolt[N] P_{m} Load absorbed by flanges[N] P_{Max} Max equivalent load in loading sequence[N] P_{Min} Min equivalent load in loading sequence[N] R_{root} Average blade root radius[m] R_{i} Blade root inner radius (Parameter)[m] $T_{default}$ Default temperature[K] W_{P} Moment of resistance[m] x^{L} Lower bounds[-] x^{U} Upper bounds[-] x^{U} Upper bounds[-] σ_{ext_max} Maximum stress due to external loading[Pa] $\sigma_{\text{bolt max}}$ Bolt stress at extreme loading[Pa] F_{pl} Bolt preload force[N] K_{joint} Stiffness of the joint[N] T_{bolt} Temperature to be applied for required prestress[K] μ_{G} Static friction coefficient[-] A_{b} Effective area of the bolt[m²]	M_{Min}	Bending moment range in a loading sequence	[Nm]
NbNumber of bolts in the blade root (Parameter) $[-]$ P External load on the joint $[N]$ $P_{\rm b}$ Load absorbed by bolt $[N]$ $P_{\rm m}$ Load absorbed by flanges $[N]$ $P_{\rm max}$ Max equivalent load in loading sequence $[N]$ P_{Min} Min equivalent load in loading sequence $[N]$ R_{root} Average blade root radius $[m]$ Ri Blade root inner radius (Parameter) $[m]$ $T_{default}$ Default temperature $[K]$ W_P Moment of resistance $[m^3]$ x Parameter set $[-]$ $x^{\rm L}$ Lower bounds $[-]$ $x^{\rm U}$ Upper bounds $[-]$ $\sigma_{\rm ext_max}$ Maximum stress due to external loading $[Pa]$ $\sigma_{\rm bolt\ max}$ Bolt stress at extreme loading $[Pa]$ $F_{\rm pl}$ Bolt preload force $[N]$ $K_{\rm joint}$ Stiffness of the joint $[N]$ T_{bolt} Temperature to be applied for required prestress $[K]$ μ_G Static friction coefficient $[-]$ $A_{\rm b}$ Effective area of the bolt $[m]$	M_{Range}	Bending moment range in a loading sequence	[Nm]
P External load on the joint $[N]$ $P_{\rm b}$ Load absorbed by bolt $[N]$ $P_{\rm m}$ Load absorbed by flanges $[N]$ P_{Max} Max equivalent load in loading sequence $[N]$ P_{Min} Min equivalent load in loading sequence $[N]$ R_{root} Average blade root radius $[m]$ Ri Blade root inner radius (Parameter) $[m]$ $T_{default}$ Default temperature $[K]$ W_P Moment of resistance $[m^3]$ x Parameter set $[-]$ $x^{\rm U}$ Upper bounds $[-]$ $x^{\rm U}$ Upper bounds $[-]$ $\sigma_{\rm ext_max}$ Maximum stress due to external loading $[Pa]$ $\sigma_{\rm bolt\ max}$ Bolt stress at extreme loading $[Pa]$ $F_{\rm pl}$ Bolt preload force $[N]$ $K_{\rm joint}$ Stiffness of the joint $[\frac{N}{m}]$ T_{bolt} Temperature to be applied for required prestress $[K]$ μ_G Static friction coefficient $[-]$ A_b Effective area of the bolt $[m^2]$	N_{bolts}	Number of T-bolts in the blade root	[-]
$P_{\rm b}$ Load absorbed by bolt[N] $P_{\rm m}$ Load absorbed by flanges[N] P_{Max} Max equivalent load in loading sequence[N] P_{Min} Min equivalent load in loading sequence[N] R_{root} Average blade root radius[m] Ri Blade root inner radius (Parameter)[m] $T_{default}$ Default temperature[K] W_P Moment of resistance[m³] x Parameter set[-] $x^{\rm L}$ Lower bounds[-] $x^{\rm U}$ Upper bounds[-] $\sigma_{\rm ext_max}$ Maximum stress due to external loading[Pa] $\sigma_{\rm bolt\ max}$ Bolt stress at extreme loading[Pa] $F_{\rm pl}$ Bolt preload force[N] $K_{\rm joint}$ Stiffness of the joint $[\frac{N}{m}]$ T_{bolt} Temperature to be applied for required prestress[K] μ_G Static friction coefficient[-] $A_{\rm b}$ Effective area of the bolt $[m^2]$	Nb	Number of bolts in the blade root (Parameter)	[-]
$P_{\rm m}$ Load absorbed by flanges $[N]$ P_{Max} Max equivalent load in loading sequence $[N]$ P_{Min} Min equivalent load in loading sequence $[N]$ R_{root} Average blade root radius $[m]$ Ri Blade root inner radius (Parameter) $[m]$ $T_{default}$ Default temperature $[K]$ W_P Moment of resistance $[m^3]$ x Parameter set $[-]$ $x^{\rm L}$ Lower bounds $[-]$ $x^{\rm U}$ Upper bounds $[-]$ $\sigma_{\rm ext_max}$ Maximum stress due to external loading $[Pa]$ $\sigma_{\rm bolt\ max}$ Bolt stress at extreme loading $[Pa]$ $F_{\rm pl}$ Bolt preload force $[N]$ $K_{\rm joint}$ Stiffness of the joint $[\frac{N}{m}]$ T_{bolt} Temperature to be applied for required prestress $[K]$ μ_G Static friction coefficient $[-]$ A_b Effective area of the bolt $[m^2]$	P	External load on the joint	[N]
P_{Max} Max equivalent load in loading sequence $[N]$ P_{Min} Min equivalent load in loading sequence $[N]$ R_{root} Average blade root radius $[m]$ Ri Blade root inner radius (Parameter) $[m]$ $T_{default}$ Default temperature $[K]$ W_P Moment of resistance $[m^3]$ x Parameter set $[-]$ $x^{\rm L}$ Lower bounds $[-]$ $x^{\rm U}$ Upper bounds $[-]$ $\sigma_{\rm ext_max}$ Maximum stress due to external loading $[Pa]$ $\sigma_{\rm bolt\ max}$ Bolt stress at extreme loading $[Pa]$ $F_{\rm pl}$ Bolt preload force $[N]$ $K_{\rm joint}$ Stiffness of the joint $[\frac{N}{m}]$ T_{bolt} Temperature to be applied for required prestress $[K]$ μ_G Static friction coefficient $[-]$ $A_{\rm b}$ Effective area of the bolt $[m^2]$	$P_{ m b}$	Load absorbed by bolt	[N]
P_{Min} Min equivalent load in loading sequence $[N]$ R_{root} Average blade root radius $[m]$ Ri Blade root inner radius (Parameter) $[m]$ $T_{default}$ Default temperature $[K]$ W_P Moment of resistance $[m^3]$ x Parameter set $[-]$ $x^{\rm L}$ Lower bounds $[-]$ $x^{\rm U}$ Upper bounds $[-]$ $\sigma_{\rm ext_max}$ Maximum stress due to external loading $[Pa]$ $\sigma_{\rm bolt\ max}$ Bolt stress at extreme loading $[Pa]$ $F_{\rm pl}$ Bolt preload force $[N]$ $K_{\rm joint}$ Stiffness of the joint $[\frac{N}{m}]$ T_{bolt} Temperature to be applied for required prestress $[K]$ μ_G Static friction coefficient $[-]$ $A_{\rm b}$ Effective area of the bolt $[m^2]$	$P_{ m m}$	Load absorbed by flanges	[N]
R_{root} Average blade root radius $[m]$ Ri Blade root inner radius (Parameter) $[m]$ $T_{default}$ Default temperature $[K]$ W_P Moment of resistance $[m^3]$ x Parameter set $[-]$ x^L Lower bounds $[-]$ x^U Upper bounds $[-]$ $\sigma_{\rm ext_max}$ Maximum stress due to external loading $[Pa]$ $\sigma_{\rm bolt\ max}$ Bolt stress at extreme loading $[Pa]$ $F_{\rm pl}$ Bolt preload force $[N]$ $K_{\rm joint}$ Stiffness of the joint $[\frac{N}{m}]$ T_{bolt} Temperature to be applied for required prestress $[K]$ μ_G Static friction coefficient $[-]$ $A_{\rm b}$ Effective area of the bolt $[m^2]$	P_{Max}	Max equivalent load in loading sequence	[N]
Ri Blade root inner radius (Parameter) $[m]$ $T_{default}$ Default temperature $[K]$ W_P Moment of resistance $[m^3]$ x Parameter set $[-]$ x^L Lower bounds $[-]$ x^U Upper bounds $[-]$ $\sigma_{\text{ext_max}}$ Maximum stress due to external loading $[Pa]$ $\sigma_{\text{bolt max}}$ Bolt stress at extreme loading $[Pa]$ F_{pl} Bolt preload force $[N]$ K_{joint} Stiffness of the joint $[\frac{N}{m}]$ T_{bolt} Temperature to be applied for required prestress $[K]$ μ_G Static friction coefficient $[-]$ A_{b} Effective area of the bolt $[m^2]$	P_{Min}	Min equivalent load in loading sequence	[N]
$T_{default}$ Default temperature $[K]$ W_P Moment of resistance $[m^3]$ x Parameter set $[-]$ x^L Lower bounds $[-]$ x^U Upper bounds $[-]$ σ_{ext_max} Maximum stress due to external loading $[Pa]$ $\sigma_{\text{bolt max}}$ Bolt stress at extreme loading $[Pa]$ F_{pl} Bolt preload force $[N]$ K_{joint} Stiffness of the joint $[\frac{N}{m}]$ T_{bolt} Temperature to be applied for required prestress $[K]$ μ_G Static friction coefficient $[-]$ A_{b} Effective area of the bolt $[m^2]$	R_{root}	Average blade root radius	[m]
W_P Moment of resistance $[m^3]$ x Parameter set $[-]$ x^L Lower bounds $[-]$ x^U Upper bounds $[-]$ $\sigma_{\text{ext_max}}$ Maximum stress due to external loading $[Pa]$ $\sigma_{\text{bolt max}}$ Bolt stress at extreme loading $[Pa]$ F_{pl} Bolt preload force $[N]$ K_{joint} Stiffness of the joint $[\frac{N}{m}]$ T_{bolt} Temperature to be applied for required prestress $[K]$ μ_G Static friction coefficient $[-]$ A_{b} Effective area of the bolt $[m^2]$	Ri	Blade root inner radius (Parameter)	[m]
W_P Moment of resistance $[m^3]$ x Parameter set $[-]$ $x^{\rm L}$ Lower bounds $[-]$ $x^{\rm U}$ Upper bounds $[-]$ $\sigma_{\rm ext_max}$ Maximum stress due to external loading $[Pa]$ $\sigma_{\rm bolt\ max}$ Bolt stress at extreme loading $[Pa]$ $F_{\rm pl}$ Bolt preload force $[N]$ $K_{\rm joint}$ Stiffness of the joint $[\frac{N}{m}]$ T_{bolt} Temperature to be applied for required prestress $[K]$ μ_G Static friction coefficient $[-]$ $A_{\rm b}$ Effective area of the bolt $[m^2]$	$T_{default}$	Default temperature	[K]
$x^{\rm L}$ Lower bounds[-] $x^{\rm U}$ Upper bounds[-] $\sigma_{\rm ext_max}$ Maximum stress due to external loading[Pa] $\sigma_{\rm bolt\ max}$ Bolt stress at extreme loading[Pa] $F_{\rm pl}$ Bolt preload force[N] $K_{\rm joint}$ Stiffness of the joint $\left[\frac{N}{m}\right]$ T_{bolt} Temperature to be applied for required prestress[K] μ_G Static friction coefficient[-] $A_{\rm b}$ Effective area of the bolt $[m^2]$		Moment of resistance	$[m^3]$
$x^{\rm U}$ Upper bounds [-] $\sigma_{\rm ext_max}$ Maximum stress due to external loading [Pa] $\sigma_{\rm bolt\ max}$ Bolt stress at extreme loading [Pa] $F_{\rm pl}$ Bolt preload force [N] $K_{\rm joint}$ Stiffness of the joint $\left[\frac{N}{m}\right]$ T_{bolt} Temperature to be applied for required prestress [K] μ_G Static friction coefficient [-] $A_{\rm b}$ Effective area of the bolt [m^2]	x	Parameter set	[-]
$\sigma_{ m ext_max}$ Maximum stress due to external loading $[Pa]$ $\sigma_{ m bolt\ max}$ Bolt stress at extreme loading $[Pa]$ $F_{ m pl}$ Bolt preload force $[N]$ $K_{ m joint}$ Stiffness of the joint $[\frac{N}{m}]$ T_{bolt} Temperature to be applied for required prestress $[K]$ μ_G Static friction coefficient $[-]$ $A_{ m b}$ Effective area of the bolt $[m^2]$	x^{L}	Lower bounds	[-]
$\sigma_{ m bolt\ max}$ Bolt stress at extreme loading $[Pa]$ $F_{ m pl}$ Bolt preload force $[N]$ $K_{ m joint}$ Stiffness of the joint $[\frac{N}{m}]$ T_{bolt} Temperature to be applied for required prestress $[K]$ μ_G Static friction coefficient $[-]$ $A_{ m b}$ Effective area of the bolt $[m^2]$	x^{U}	Upper bounds	[-]
$F_{ m pl}$ Bolt preload force [N] $K_{ m joint}$ Stiffness of the joint $\left[\frac{N}{m}\right]$ T_{bolt} Temperature to be applied for required prestress [K] μ_G Static friction coefficient [-] $A_{ m b}$ Effective area of the bolt [m ²]	$\sigma_{ m ext_max}$	Maximum stress due to external loading	[Pa]
$K_{ m joint}$ Stiffness of the joint $\left[\frac{N}{m}\right]$ T_{bolt} Temperature to be applied for required prestress $\left[K\right]$ μ_G Static friction coefficient $\left[-\right]$ $A_{ m b}$ Effective area of the bolt $\left[m^2\right]$	$\sigma_{ m bolt\ max}$	Bolt stress at extreme loading	[Pa]
T_{bolt} Temperature to be applied for required prestress $[K]$ μ_G Static friction coefficient $[-]$ $A_{\rm b}$ Effective area of the bolt $[m^2]$	$F_{ m pl}$	Bolt preload force	[N]
T_{bolt} Temperature to be applied for required prestress $[K]$ μ_G Static friction coefficient $[-]$ $A_{\rm b}$ Effective area of the bolt $[m^2]$	$K_{ m joint}$	Stiffness of the joint	$\left[\frac{N}{m}\right]$
$A_{ m b}$ Effective area of the bolt $[m^2]$		Temperature to be applied for required prestress	
$A_{ m b}$ Effective area of the bolt $[m^2]$	μ_G	Static friction coefficient	[-]
$A_{\rm jm}$ Effective area of the joint members $[m^2]$		Effective area of the bolt	$[m^2]$
	$A_{ m jm}$	Effective area of the joint members	$[m^2]$

d_0	Bolt shank diameter	[m]
d_2	Pitch circle diameter of the thread	[m]
$E_{ m b}$	Smeared Young's modulus of the bolt	$\left[\frac{N}{m^2}\right]$
$E_{ m jm}$	Smeared Young's modulus of the joint members	$\left[\frac{N}{m^2}\right]$
$F_{ m bolt}$	Force in the bolt	[N]
$l_{ m b}$	Effective length of the bolt	[m]
$l_{ m jm}$	Effective length of the joint members	[m]

xxii List of Symbols

Preface

This project is a part of my Master of Science graduation thesis and is my very first attempt at the optimization procedure. The design process at Suzlon has focused on delivering designs for the blade root with detailed structural and fatigue analysis. Over time the blades and towers have increased in size, and the designs have gotten bulkier as is expected from the design evolution of wind turbines. Thus the blade roots have to endure increasingly large loads, and the geometry of the blade root has given rise to local bending of the laminate and T-bolts. The engineers suspected that due to bending loads in the T-bolts they were not able to utilize the T-bolts to their maximum capacity. This called for an investigation into the joint and perhaps a minor redesign or change in the direction of design procedure to attempt utilizing the materials in the blade root better. After multiple rounds of interaction with the Supervisors, the aim of optimization to minimize cost and other sub-goals matured.

This thesis was a great learning experience and a description of both the quantifiable and the conceptual aspects of optimizing a structure will be presented. A philosophy of optimization or the guiding principle is outlined that will help future attempts at the same conclude with meaningful and substantial results. Optimization is a trade off process, and this is known to the veterans of the field. While attempting to minimize the cost of a structure, the material is removed, and this will make one or more of the many parts of a system progressively more critical. We, humans, are capable of mitigating this by adapting to the conditions, but complex algorithms cannot adapt and declare convergence with practically inadequate cost reduction! Thus it is important, first, to push the design away from the walls of constraints and then initialize the optimizer. This concept will be one of the founding principles for optimizing the blade root.

In this report the chronological steps taken to achieve a theoretical savings of nearly 13% of Reference design cost per blade root is presented. Initially, all the existing knowledge in the relevant fields are presented as a literature survey followed by the central research questions that will lay the foundation for the thesis project. Next, the finite element model and the conceptual frame work used for optimization and the structure of the various functions and various mathematical formulas employed in the calculations is presented. This is followed by a concise description of the optimization process and resulting design with its benefits. Finally, all the results are compiled, and their direct and indirect implications on manufacturing and maintenance are discussed in detail followed by the answers to the research questions.

xxiv

Acknowledgments

I would like to thank my supervisor and mentor at TU Delft, Dr.ir. Sonell Shroff for her endless assistance during this thesis. I would also like to thank her for helping me make an informed decision about my future! Thank you for helping me and supporting me through my masters and for the supporting words when I was convinced I had messed up!

I would like to thank Professor Christos Kassapoglou for his invaluable 'two cents' worth in the time of great stress!

I would like to thank my supervisor and mentor at Suzlon, Mr Valter Bellotto for the guidance and support he has provided me. His persistent belief that it could be done, got it done!

I want to thank all my professors at TU Delft for all their lectures and contributing invaluably to what I am and will be.

I want to thank Mr. Ratan Agarwal, and Mr and Mrs Mishra, for teaching me to be a finer human being when I needed it the most!

Thanks to my great friend and colleague Shreya for keeping me focused and helping me through all the intellectual crises! You are one hell of a friend!

Thank you Anjana Rao for secretly missing me from back home! You are the coolest sister ever! I hope to be in your acknowledgments page some day!

Thank you Grandma and Grandpa for dedicating your life to us. You built me with your own hands.

And, thanks mom and dad for reminding me daily from 7748 Kilometers away, of the brighter and more important things in life! For reminding me to be happy. For telling me that there is nothing to worry about. And that everything is fine!

Delft, University of Technology 14/9/2017

Athul Narayana Rao

"You are our son and you cannot fail!"

— Mom and Dad

Introduction

A turbine blade is subjected to various loads with the most significant ones being its self-weight and the wind loads. These loads have resulting moments which the blade root must endure and resist. As the turbine rotates, the moment due to its self-weight varies in a sinusoidal manner. It is also the biggest contributor to fatigue loading. Turbulence in the wind also causes disturbances in the loads resulting in additional fatigue loading cycles. In practice, the sensors mounted on the blades are monitored, and the data are recorded so a better picture of the fatigue loading can be gained.

Recent investigation has shown that these loads combined with the geometry of the blade root and hub has given rise to undesirable local bending stresses in the root laminates. In this chapter, the general geometry of the blade root will be presented to illuminate the motivation for the underlying hypothesis by the engineers at Suzlon Blade Technology (SBT), and subsequent problem statement from Suzlon. The research objective will then be presented.

1.1 The blade root connection

The wind turbine is controlled based on a variety of factors. Maintenance and other repair work require the turbine be brought to a complete stop. If the turbine is designed to function above its first bending natural frequency, generally called the soft-soft design, then low wind speeds might slow down the turbine enough to cause resonance and high bending moments on the base. To avoid such behavior, a control system is installed that continually measures wind speed and direction and adjusts the angle of attack of the blade to achieve the desired effect. Thus it is necessary that the blade is connected to the hub via bearing that will allow axial rotation of the blade in the plane of the turbine. This bearing is visible in Figure 1.1.

This bearing is a heavy duty slew bearing with either 1 or 2 race ways for the bearing balls depending on the design requirements. A schematic of this bearing is shown in Figure 1.2. In the design focused on in the project, there are two raceways.

2 Introduction

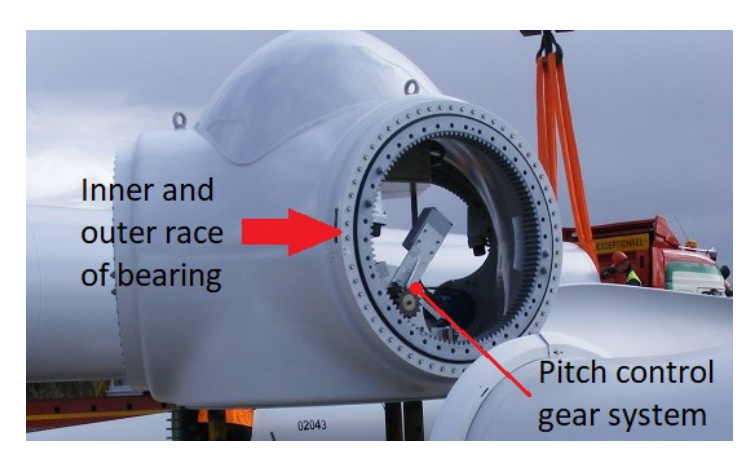


Figure 1.1: Blade root-hub bearing and pitch control gear system [1].



Figure 1.2: Hub slew bearing [2].

Due to wind loading and self-weight of the rotating blade, there is a large bending moment that the hub bearing must resist. This bending moment appears as loads on the inner race of the bearing which is transferred to the outer bearing via the bearing balls.

The rotor blade is made from Glass Fiber Reinforced Plastic (GFRP) composite sandwich often with balsa wood core with I-section stiffeners acting as the primary lateral load carrying structure and hat stiffeners to prevent the buckling of the skin. This aerodynamically optimized part of the blade is attached to the hub through the blade root which is a cylindrical section with an unusually thick laminate with a thickness of over 100mm. This increase in thickness is to compensate for the holes drilled for the T-bolt barrel-heads. During service, the blade root will be subjected to bending, shear and axial loads. To prevent premature bending of the blade root, a circumferential stiffener is provided. This stiffener also doubles up as a platform for the maintenance personnel to stand on for inspection of the T-bolt assembly and the pitch control mechanisms.

The outer race of the bearing is connected to the hub which is made of metal via an additional set of bolts aligned similarly to the T-bolts in the blade root. This is an important connection for the blade root as it determines the boundary conditions while studying the behavior of the blade root.

1.2 Problem statement by Suzlon and research objective

The bearing and hub flexibility combined with the offset in the load path has given rise to local bending moments at the T-bolt joint which causes joint opening at the T-bolt connection and bending of the T-bolt shank. This results in an unexpected nonlinear behavior of the blade root connection which drastically affects the fatigue life under extreme loading cycles. It is hypothesized that this nonlinear behavior can be reduced by modifying the design of the blade root. Reduced stresses appearing at the bolt shank will allow better utilization of the bolt design. To achieve reduced stress and local bending at the T-bolt shank, the blade root connection must be structurally optimized.

The research will identify a set of parameters which can be used to manipulate the design of the blade root connection to achieve a better performing design while respecting the various design constraints that are identified in the literature survey. A set of generalized design guidelines will be drawn that can aid in the optimization of the blade roots that will be developed in the future.

Thus the research objective is to "Outline a set of design guidelines and recommendations to optimize and simplify the blade root by: (a) analyzing the finite element model of the blade root and (b) identifying key design parameters to aid the optimization process and (c) searching for an optimized design by employing a robust algorithm".

4 Introduction

1.3 Reader's guide

The thesis report, henceforth, is divided into 4 chapters. They are listed below, and the content and intent are discussed.

- Literature survey and theoretical foundations This chapter presents the existing research and knowledge in the fields relevant to the subject of the thesis, which is the optimization of a blade root connection. It will discuss the broad topics of joints and its types, forces, and stresses on the blade root, failures of bolted joints, and optimization problems. This chapter will be concluded by laying the theoretical foundation for the thesis work by outlining the research questions.
- Finite element model and optimization framework This chapter will discuss the original finite element model of Suzlon, its construction, loads and boundary conditions. It will discuss the modifications done on Suzlon's model for the thesis work. After presenting the FEM framework, the optimization framework is presented.
- **Optimization** The chapter encapsulates the entire process of optimization from the preparation to the convergence and describes the improvements achieved in the final Optimized design.
- Results The chapter discusses the results of the optimization process, the technical and conceptual takeaway, the implications of the design modifications and presents the conclusions and recommendation for the design of the blade root.

Literature survey and theoretical **foundations**

In this chapter, the relevant literature, research, and theoretical foundations are presented. The types of connection, mathematical definitions, loads, failure modes and other necessary fields will be introduced and discussed. Finally, the central research questions are presented that will lay the foundation to the thesis work.

2.1 The T-bolt connection

T-bolts or more popularly known as the Ikea bolts are designed for connections where access to the bolt is possible only from one side thus making it necessary for the bolt itself to be able to arrest its axial rotational degree of freedom. This is done by designing one end of the bolt with a barrelhead perpendicular to the bolt itself which can be screwed on. The axis of the T-bolt is parallel to the axis of the root laminate and generally at the center of the laminate, and the barrel head sits perpendicular to the laminate and in radially drilled holes. The geometry of the bolt and its placement in the laminate is presented in Figure 2.2. The tightening of the T-bolt will cause compressive contact stresses at the root-bearing interface which is an important feature for resisting the loads.

2.2 **Fatigue in bolted connections**

Bolted connection in general consists of the bolt itself and the components being joined. After tightening the bolt experiences a tensile force. This tensile force produces compressive force in the material of the components being held together by the bolt, referred to here as flanges, although the geometry can be different. This creates a system of stiffness as modeled by Martinez et al. in 2001 [3]. Loading the joint results in the distribution of the load between the bolt and the flanges. The fraction of external load appearing on the bolt as an increase in stress above the pretension stress is dictated by the geometry of the joint and the material properties.

Eq. (2.1) shows a conceptual linear relationship between the joint stiffness and the components of the joint. It can be observed that the fraction of the load taken up by the components i.e. bolt or flanges is proportional to their fractional contribution to the joint stiffness.

$$K_{\text{joint}} = \underbrace{\frac{E_{\text{jm}}A_{\text{jm}}}{l_{\text{jm}}}}_{\text{Joint member's contribution}} + \underbrace{\frac{E_{\text{b}}A_{\text{b}}}{l_{\text{b}}}}_{\text{Bolt's contribution}}$$
(2.1)

Here, K_{joint} is the conceptual stiffness of the joint. E_{jm} , A_{jm} and l_{jm} are the Young's modulus, cross-sectional area, and length of the joint members or the flanges inside the stress cone of pretension. E_{b} , A_{b} , and l_{b} are the Young's modulus, cross-sectional area, and length of the preloaded bolt, respectively.

The load on the joint is resisted by the relaxation of the flanges and the tensioning of the bolt. The load appearing on each joint member, i.e. flanges and bolts, is proportional to their stiffness contribution to the joint, and this follows Eq. (2.1). Thus, a joint with a stiffness dominated by the flanges will show better fatigue properties compared to a joint with bolts dominating the stiffness, because fatigue is often more critical in members experiencing tensile loading, as the bolt. Thus, while designing the bolted joint at the blade root stress analysis at the loads prescribed by the Det Norske Veritas (DNV) Germanischer Lloyd (GL) guidelines [4] is carried out, and the joint is often optimized for adequate fatigue life with the lightest design.

The fatigue properties of a bolt are also influenced by the type of the thread used. Since a detailed analysis of the effects of using different threads and the influence of the thread itself is outside the scope of this project, the European standard for the design of steel structures [5] is referred for the SN curve that is derived from the study of bolts.

2.3 Optimization of bolted connection

The concept of optimization of bolted connection is treated as a multivariate optimization problem to provide a holistic approach to it. Optimization can be carried out for a number of variables like the mass, cost, fatigue life, stresses, etc. Choosing one variable alone will inevitably over design the structure. Thus it is important to select appropriate design parameters that will provide an effective manipulation set for the performance of the bolt while preventing over design and expensive components.

The simplification of design is a highly subjective term it can be viewed as a simplification of manufacturing complexity or even simplification of maintainability and repairability. Often the interests are conflicting. For example one might expect a simple design to include reduced number of bolts with increased size of bolts so that the number of holes drilled is lesser but larger bolts make repairs tougher as taking heavy bolts to the height of a blade will require considerable effort, and it might need the personnel to put in more effort to tighten them.

One of the most important factors in a wind turbine is the mass. Reduction of weight of the blade root while keeping the fatigue life in check can prove to be beneficial. This will also

result in a reduction of cost. Minimizing the number of holes drilled through the composite laminate can help in reducing potential sites of crack nucleation and probability of laminate damage while also reducing machining time.

2.4 Blade root connection - Popular designs

In general, there are two major designs that are in use today for the blade root connection. Both these designs are aimed at connecting similar kinds of structures together. Most popularly the cylindrical laminate of the blade root will be butt joint to the circular slew bearing's inner race using an embedded bolt. This embedded bolt can either be a T-bolt, where the shank is inserted parallel to the laminate at its center, coaxial to the blade root that screws into the barrel head placed along the radial direction of the laminate as shown in Figure 2.2.

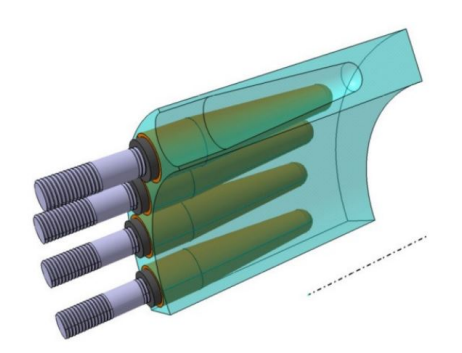


Figure 2.1: Bushing connection [6].

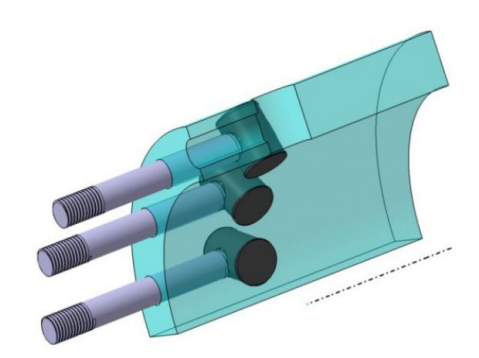


Figure 2.2: T-bolt connection [6].

The bushing connection relies on the shear strength of the bond between the bushing and the laminate, whereas, the T-bolt connection relies on the contact between the barrel head and the laminate for transferring the load. The bushing connection is shown in Figure 2.1.

Blade root with T-bolts is the design currently employed by Suzlon in most of its wind turbines. The exact definition of the T-bolt connection at the blade root and its features ascertain its exact use in the blade root, and there is exhaustive documentation of this made available by the European patent office [7].

2.5 Forces and stresses at blade root connection

The most dominant force at the blade root connection is the stress due to the wind and self-weight. The loads due to self-weight are periodic and follow the frequency of the turbine, compared to the random loading by the wind, which is a result of the turbulence. All these force result in different stress states at the blade root. The cumulative effect of the loads can be approximated as a bending moment at the blade root that causes tension-compression stresses to develop at the blade root. This stress has to be resisted by the hub and since there is a bearing that holds the blade root to the hub the forces at the blade root must first be transferred into the bearing, and then the bearing must transmit it further. The bearing produces an offset in the path of the load, and this is because the root is attached to

the inner race and the hub, to the outer race. An offset in the load path gives rise to local bending moments as can be seen in most lap joints. The local bending moments in the blade root causes localized bending of the laminate at the blade root and similar bending of the bearing races. This naturally translates to increased tensile stresses in the bolt shank which has adverse effects in both the design of the blade root and the fatigue life.

Other forces include the shear forces caused by the self-weight and other intermittent loads by the random turbulence in the wind. All these loads contribute to the fatigue loading of the joint and the laminate.

2.6 Composites general information

A laminate of a fiber reinforced plastic consists unidirectional plies or bidirectional weaves of high strength fibers that are stacked on top of one another and are unified using the resin or matrix via processes like vacuum infusion. The stiffness of these laminates is highly customizable by controlling the orientation of the weaves. The most traditional method of tabulating the stiffness of a laminate is using the ABD matrix [8].

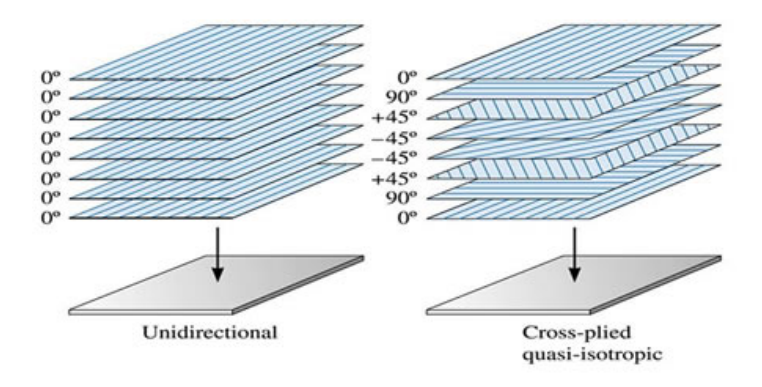


Figure 2.3: Stacking sequence - unidirectional vs isotropic [9].

The root laminate of the blade is generally a quasi-isotropic laminate [8]. An example of this is shown in Figure 2.3. A quasi-isotropic laminate has properties similar to an isotropic material in all loading directions in the plane of the laminate. Any deviation from a quasi-isotropic layup will produce an orthotropic layup which has two distinct Eigen directions of minimum and maximum stiffness in the plane of the laminate.

The bending stiffness of the laminate can be increased by increasing the local stiffness of the plies furthest from the center of the laminate [8]. This is done by applying 0° plies at the beginning and end of the laminate, thickness wise. The directions of the plies are shown in Figure 2.4.

Another popular blade root laminate layup is the Triax layup. This constitutes plies in a repeating pattern of 0° , $\pm 45^{\circ}$. the 0° ply is predominantly unidirectional ply with a few 90° fibers meant to hold the 0° fibers together. The $\pm 45^{\circ}$ is a weave and has an equal number of $+45^{\circ}$ and -45° fibers.

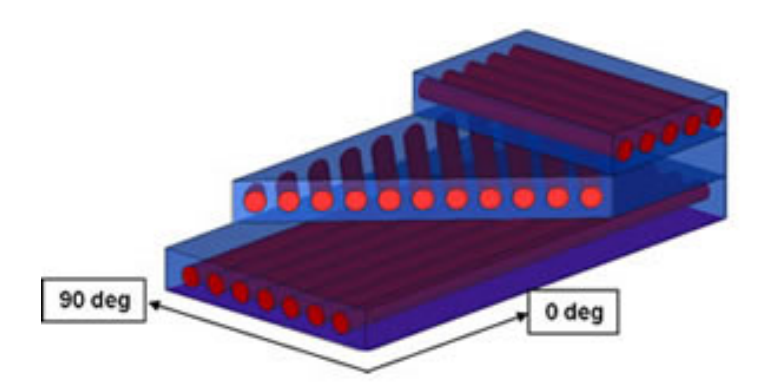


Figure 2.4: Ply directions [9].

2.7 General composite failure modes

The failure of the composite laminates can be studied either micromechanically or macro mechanically. Although the micro mechanics is what governs the macro mechanical properties, the latter usually provide more meaningful and useful data while manufacturing and testing for mass production.

Composite bolted joint fail often in the same modes as other similarly bolted joints. There are four modes of failure in the laminate that are relevant while designing a composite bolted joint [10].

- 1. Bearing failure
- 2. Net-section failure
- 3. Shear-out failure
- 4. Cleavage failure

Hodgkinson et al. [11] have presented several failure analysis and data from Fiber Reinforced Plastic (FRP) laminates. The most prominent modes of failure in the laminates have been found to be shear out, net section and bearing failures in specific geometric conditions. These laminate failures are prevented by ensuring the following inequalities are respected in the model during the most adverse loading state.

$$\sigma_{\text{ut_comp}} > \frac{F_{\text{bolt}}}{A_{\text{bearing}}}$$
 (2.2)

Eq. (2.2) is condition for checking bearing failure. $\sigma_{\rm ut_comp}$ is the ultimate compressive strength of laminate in the direction of force, $F_{\rm bolt}$ is the tensile force in the bolt and $A_{\rm bearing}$ is the bearing area in the laminate.

$$\sigma_{\text{ut_tens}} > \frac{F_{\text{bolt}}}{A_{\text{netsection}}}$$
 (2.3)

Eq. (2.3) is condition for checking net-section failure. $\sigma_{\text{ut_tens}}$ is the ultimate tensile strength of laminate at the net section plane and $A_{\text{netsection}}$ is the net-section area of the laminate

between bolts.

$$\sigma_{\text{ut_shear}} > \frac{F_{\text{bolt}}}{A_{\text{shearout}}}$$
 (2.4)

Eq. (2.4) is condition for checking shear-out failure. $\sigma_{\rm ut_shear}$ is the ultimate shear strength of laminate in the direction of force and $A_{\rm shearout}$ is the shear area corresponding to the bolt.

The stress planes referred to in Eq. (2.2), Eq. (2.3) and Eq. (2.4) are shown in Figure 2.5 which depicts the vicinity of a pin loaded hole in a rectangular laminate.

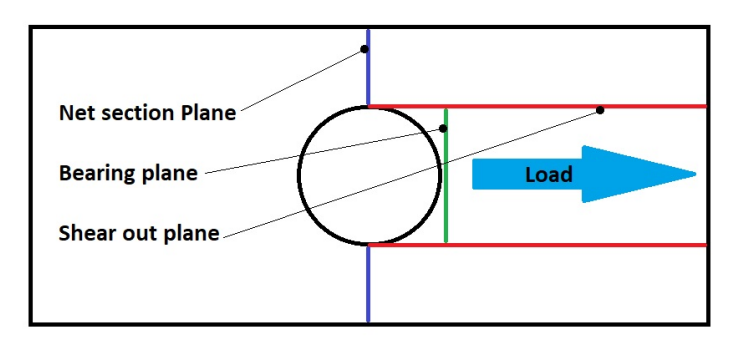


Figure 2.5: Stress planes [10].

The barrel head acts as a pin that loads the composite via the bearing plane. Usually, pin loaded joints are present with a nut and a washer providing pretension in the pin that helps increase the effective bearing area. The barrel head has no such nut and washer and thus has a much lower bearing area compared to other bolted joints. The composite failure modes in pin loaded joints along the planes described in Figure 2.5 are shown in Figure 2.6.

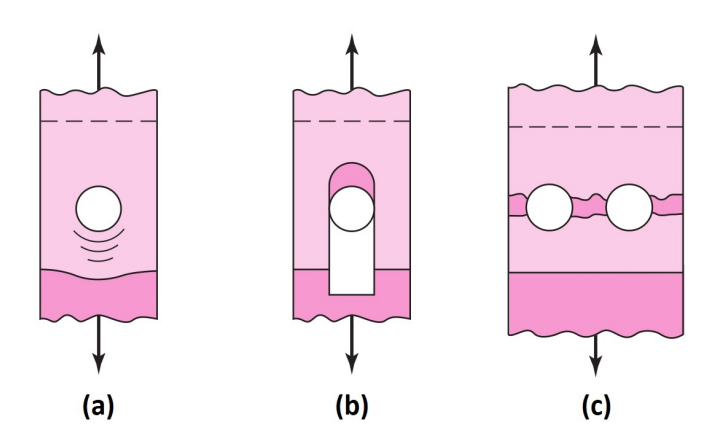


Figure 2.6: Bolted joints failure modes (a) Bearing (b) Shear out and (c) Net section failure [12].

2.8 Bolted joints

Bolted connections can broadly be classified into two categories, the joints loaded in shear and the joints loaded in tension.

2.8 Bolted joints

2.8.1 Shear loaded bolted joints

The shear loaded joints make use of the bolt preload to induce adequate friction between the members being joint. This friction prevents all the load being transferred via the bolt. Allowing load transfer via friction reduces the criticality of the failure modes depicted in Figure 2.6. Figure 2.7 shows the modes of failure in the rivet loaded in shear which is effectively similar to the joint involving bolts. The members being joined are positioned parallel to each other. And the bolts are inserted and tightened to increase contact forces. These contact forces increase the maximum friction force allowed. A part of the external load is transferred via shear of the bolt, and the remainder is transferred via friction between plates. The bolt is accessible from both sides making it easy for the personnel to hold one end and tighten the other.

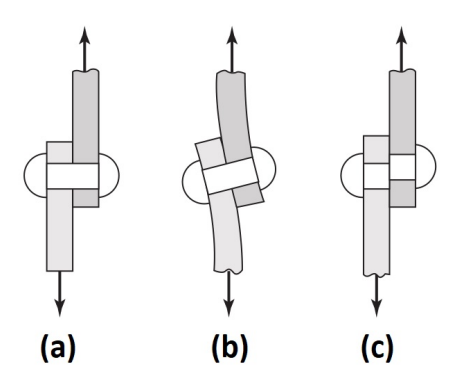


Figure 2.7: Bolt/rivete failure modes (a) Loading direction (b) Secondary bending (c) Shearing of bolts [12].

Figure 2.8 shows a condition where access to the bolt is limited from one side only. In such case, T-bolts could be indispensable. Welding is not an option here as the structures are designed to have variable height and welding is a permanent joining technique.



Figure 2.8: T-Bolt with limited access [13] [14]

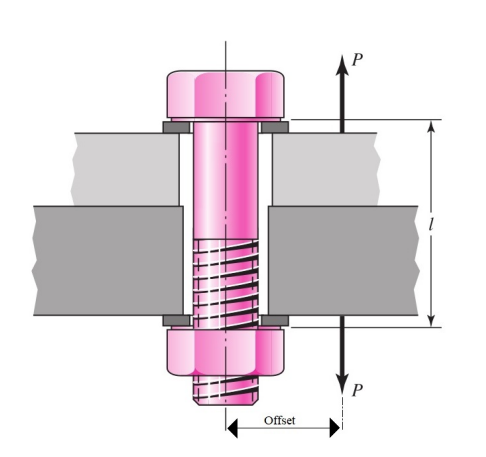
The remote end of the bolt will lock itself into a grove on the inside of the vertical shaft shown in blue in Figure 2.8. This particular T-bolt is loaded in shear. For the analogous example in

composite wind turbine blade root refer to Figure 2.2. T-bolts are particularly useful when the components being connected are perpendicular to each other as shown in Figure 2.10.

The remote end is the barrel-head. The design of the bolt is such that the barrel-head's rotation about the axis of the shank is arrested by the surrounding laminate and similarly the position of the bolt is also arrested. Thus the person attempting to tighten the nut is able to do so without added help. The shank is often long and slender thus these bolted joints are not intended for transmitting bending loads although small amounts of bending loads as a result of the geometry are often inevitable. These are taken into consideration while designing the joint.

2.8.2 Tension loaded bolted joint

Tension loaded bolted joints are commonly found in flanges and roof attachments. The preload applied to these bolts are critical when the members being joint are supposed to transmit time varying loads [15]. Most bolted joints loaded in tension have the load introduced into the bolt-plate joint from a point or axis slightly shifted from the stiffness axis of the bolt itself and, thus, it experiences some amount of bending as is. The offset between the axis of loading and the axis of the bolt can be seen in Figure 2.9.



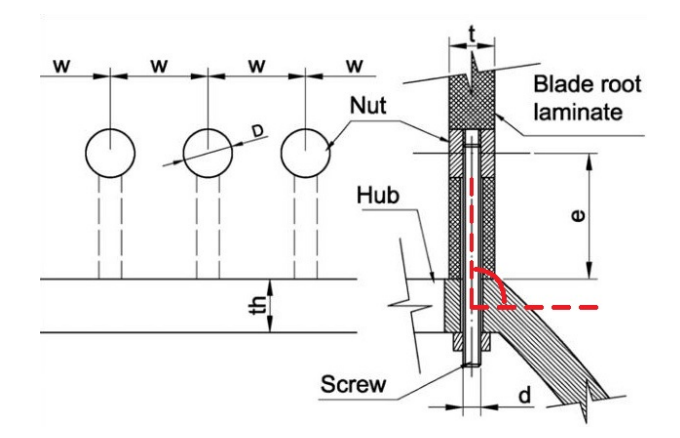


Figure 2.9: Bolt loaded in tension [12]

Figure 2.10: Perpendicularity of members in T-bolt connection [16]

Since the members being joined are not parallel, evident in Figure 2.10, bending loads appear at the joint. A bearing is placed between the root and the hub and is not shown in Figure 2.10. The utility of this bearing is explained in Section 1.1.

Joint separation is an important design criterion for tension loaded joints. The pretension of the bolt unifies the bolt and plates into a joint and this joint has a stiffness that is a combined stiffness of the bolt and plate in parallel. The pretension of the bolt is balanced by the compression in the plates that also appears as contact stresses at the plate-plate interface. On application of external load this stress reduces and the bolt force increases. The fraction of the external load absorbed by the bolt and composite is dictated by the two separate contributing terms on the Right Hand Side (RHS) in Eq. (2.1), which can be simplified as given in Eq. (2.5).

2.9 T-bolt joint

$$K_{\text{joint}} = K_{\text{bolt}} + K_{\text{joint material}} = K_{\text{b}} + K_{\text{m}}$$
 (2.5)

 $K_{\rm joint}$, $K_{\rm b}$ and $K_{\rm m}$ are the theoretical axial stiffnesses of the joint, bolt and the joint material, also called the flanges. Victor Martinez et al. [16] provides the following explanatory expression given by Eq. (2.6) to calculate the load absorbed by the bolt. The term Φ in Eq. (2.6) is called the bolt stress ratio and is typically between 0.16 and 0.25 for common bolted joints [16].

$$\Delta F_{\rm b} = P_{\rm b} = \frac{K_{\rm b}}{K_{\rm b} + K_{\rm m}} P = \Phi P$$

$$P_m = (1 - \Phi)P \tag{2.6}$$

 $P_{\rm b}$, $P_{\rm m}$, P and Φ are the load absorbed by the bolt, load absorbed by flanges, external load on the joint and the stress ratio of the joint respectively. The behavior of the stress in the bolt and surrounding material is schematically shown in Figure 2.11.

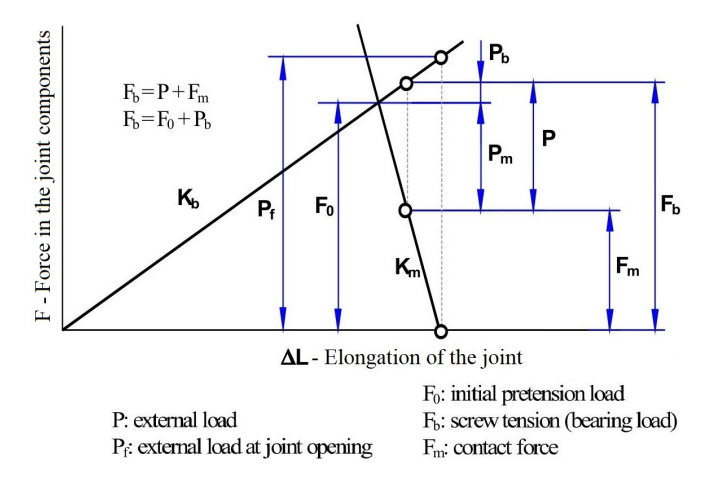


Figure 2.11: Bolted joint working diagram [3]

An increase in the external load applied denoted by P will lead to a reduction in the compressive load in the composite by P_m and increase in the tensile load in the bolt by P_b . It is advisable to decrease the contribution of the bolt to joint stiffness to reduce the fatigue loading of the bolt.

2.9 T-bolt joint

2.9.1 T-bolt properties and parameters

T-bolts, or more popularly known as the Ikea bolts, have a variety of designs as can be seen from the contrast in designs in Figure 2.8 and Figure 2.10. The former is intended for shear loading and the members being joint are parallel to one another. The latter joins members that are perpendicular to each other. Thus, the end with the barrel head will be embedded

inside the volume of one of the members being joined as shown in Figure 2.10 which also shows the different parameters that define the bolt itself. As every other bolted joint, the inter-bolt spacing or the period of the bolts 'W' is important. A large 'W' will cause the joint to separate prematurely, and a small value for 'W' will cause net section failure in the laminate. Other important parameters include the diameter of the bolt 'D' and distance of the barrel head holes from the edge of the laminate 'e'. Parameter 'd', the diameter of the shank, plays a major role in the fatigue performance of the joint. Parameters 'e' and 'th' play a major role in determining the length of the shank which directly influences the stiffness of the bolt, that is denoted by ' K_b ' in Figure 2.10 and Eq. (2.6).

2.9.2 Stresses in a T-bolt

Tension loaded T-bolt joints are subject three principal stresses.

- 1. The tension from the pretension and the external loading.
- 2. The torsion from the tightening of nut for application of pretension.
- 3. The bending stresses appearing as a result of secondary bending of the joint.

These stress and their superimposition are shown in Figure 2.12, which depicts only the forces in the axial direction. There exists a shear force in the tangential direction at the circumference of the bolt. This is due to the torquing of the bolt for pretension.

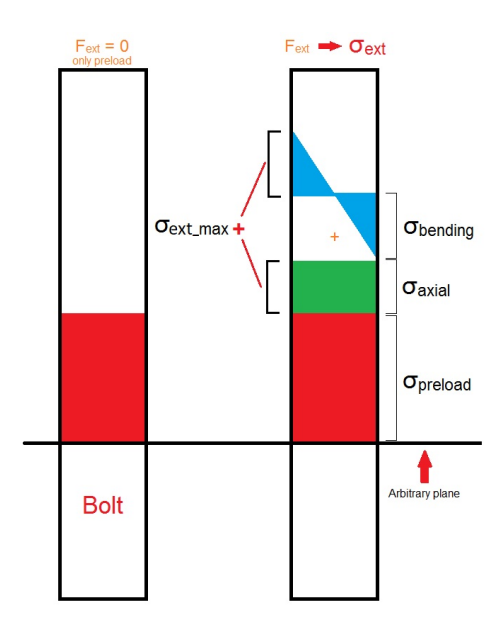


Figure 2.12: Axial stresses in bolt

The most critical point along the periphery of the bolt is the point where all the forces superimpose in the same direction. The pretension is applied such that the axial stress caused by it is 540MPa and the torsion shear stress appearing in the bolt due to this tightening is given in Eq. (2.7), provided by the German heavy duty bolt standard [17].

2.9 T-bolt joint

$$\tau = \frac{M_{\rm g}}{W_{\rm p}} \tag{2.7}$$

 τ is the shear stress generated in the bolt shank due to torquing, M_g is the moment applied to torque the bolt, given by Eq. (2.8), and W_P is the moment of resistance of the bolt shank.

$$M_{\rm g} = F_{\rm pl} \left(\frac{p}{2\pi} + 1.155 \mu_G \frac{d_2}{2} \right)$$
 (2.8)

In Eq. (2.8) p is the pitch of the thread and d_2 is the pitch circle diameter of the thread. $F_{\rm pl}$ is the preload force which can be derived from the pre-set value of the preload stress of 540MPa. μ_G is the static friction coefficient typically 0.09 for steel [17], at the thread interface between nut and bolt. The torsional resistance of the $W_{\rm p}$ is given by Eq. (2.9), where, d_0 is the bolt shank diameter.

$$W_{\rm P} = \frac{\pi}{16} d_0^3 \tag{2.9}$$

The check for the static safety of the bolt is done using the Von Mises criteria at the shank of the bolt given by Eq. (2.10). σ_{yeild} is the yield stress of the bolt and $\sigma_{\text{ax_total}}$ is the maximum tensile stress in the bolt.

$$\frac{\sigma_{\text{yeild}}}{1.1} > \sqrt{(\sigma_{\text{ax_total}})^2 + \tau^2}$$
 (2.10)

Where,

$$\sigma_{\text{ax_total}} = \sigma_{\text{pl}} + \sigma_{\text{ext_max}} = \sigma_{\text{pl}} + \sigma_{\text{axial}} + \sigma_{\text{bending}}$$
 (2.11)

 $\sigma_{\rm pl}$ is the tensile stress of preload and $\sigma_{\rm ext_max}$ is the highest stress increase due to external loading which can be split into $\sigma_{\rm axial}$ and $\sigma_{\rm bending}$, that represent the axial and bending stress due to external loading respectively. The axial and bending stresses are shown in Figure 2.12. The preload stress is considered to remain constant throughout the life of the bolt. The stresses due to external loading contribute to the fatigue loading of the bolt.

2.9.3 Maximum expected load

From past studies and analyses at Suzlon, it is found that the reference design of the blade root is expected to resist a maximum of 10.5MNm of bending moment. This is the worst case scenario and is expected to occur very rarely. This load will be referred to as the maximum expected load and is not a constant. It will vary depending on the design of the turbine.

2.9.4 Fatigue analysis

In the early stages of the thesis, to ensure the stresses do not radically exacerbate and cause fatigue loading, the $\sigma_{\rm ext_max}$ stress in the bolt is extracted when the damage equivalent load of 3MNm is applied and this stress is ensured to be lesser than the corresponding stress in the

Reference design. An approximate check for fatigue loading is done by treating $2 \times \sigma_{\text{ext}_{\text{max}}}$ as the stress range in the bolt and finding the allowable number of cycles from the SN curve given in Figure 2.13. The allowable number of cycles must be strictly above 10 million, which is the number of expected cycles of the damage equivalent load. The SN curve for the equivalent constant amplitude loading is taken from the Euro Standard [5] and curve is mathematically defined by DNV [18].

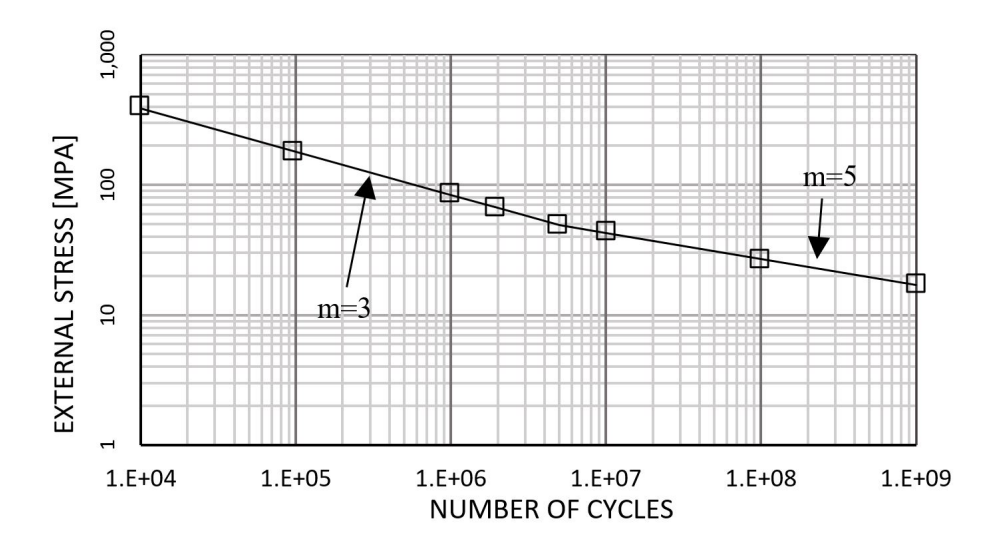


Figure 2.13: SN line from EN1993-1-9-2005 standard [5]

2.10 Optimization problems

Broadly optimization can be categorized as optimization where the derivative is known and optimization where the derivative is unknown. The second types of problems are also known as black box optimization. A black box is a form of problem where a set of inputs is provided to an extensive system of operations or functions that return an output. The intermediate steps are either unknown or far too complicated to be interpreted or approximated as an algebraic equation.

Mathematically the process of optimization is to either maximize or minimize a function (f(x)) of a set of parameters (x), while obeying a set of constraints of inequalities $(g_i(x))$ and equalities $(h_i(x))$ inside a bounded region defined by the upper (x^{U}) and lower bounds (x^{L}) . This is represented mathematically in Eq. (2.12). The function to be minimized is often referred to as the cost or loss function and if its maximization that we have to carry out then, it's called the health or fitness function. But these functions are interchangeable because minimization of a function is equivalent to maximization of its negative.

minimise
$$f(x)$$

constraints: $g_i(x) > 0$ & $h_i(x) = 0$
 $i = 1, 2...n$
for $x^L \le x \le x^U$ (2.12)

Optimization of a mathematical function is just one aspect of an engineering problem. The choice of the suitable parameters and cost functions are essential for meaningfully optimizing a design. In the most general sense optimization of design will aim for lower mass, cost, and complexity. The term complexity is subjective and must be interpreted in the context of the problem. In the case of a blade root, reducing the number of bolts can result in a reduction of complexity. Similarly, a thicker root will require more plies, thus, higher complexity.

2.10.1 Basic framework

While optimizing a design, usually a Finite Element Method (FEM) model is used. This FEM model is either a full model or a reduced model with appropriate symmetry boundary conditions applied. A script is prepared that calls the optimizing algorithm. The optimization algorithm then iteratively solves for the most optimized solution. At each iteration, a new set of parameters is passed to the FEM program which creates the model, solves it and returns data back to the algorithm for the calculation of the fitness function. Immediately after this, the constraints are checked. This process is continued till a convergence criterion is met.

2.10.2 Constraints

The constraints in an engineering problem are usually the stresses in the members and other failure loads and design thumb-rules. In the case of the blade root, as described in Section 2.9.1, parameters can have a large influence in the stresses appearing in the system. Reduction in the number of bolts in a given blade root will cause the net-section stresses in the laminate to decrease, but the stresses in the bolts will become increasingly critical. A large number of bolts will reduce the net section area and will require a thick laminate to compensate. Thus net-section stress, shear-out stress, bearing stress and the bolt stress are all a part of the constraints, and they must not exceed their design limits, which is provided as an input from Suzlon. The fatigue life of the bolt will be strictly maintained above 20 years, as this is the preset value. This will also be a constraint. From prior investigation done at Suzlon, the damage equivalent bending moment is found to be 3MNm of torque which produces the Damage Equivalent (DaEq) stress given in Table 2.1. Thus the range of stresses appearing at the bolt when subject to 3MNm of bending load must allow for a fatigue life above 20 years. To ensure this a safety factor of 1.15 is applied to the stress amplitude in the bolt.

	Ultimate limit	Safety Factor	Design limit
	MPa	[-]	MPa
Net-section stress	480.0	2.20	217.2
Bearing stress	220.0	2.20	99.5
Shearing stress	200.0	2.20	90.5
Bolt stress	900.0	1.10	818.2
DaEq Stress	24.0	1.15	20.78

Table 2.1: Design limits of constraint stresses (Courtesy: Suzlon Energy Ltd.)

2.10.3 Programming environments

Open sourced freely available algorithms, and callable function in environments like Python and MATLAB provides a simple yet powerful tool to optimize black box functions. Both these platforms offer only to minimize a function and treat maximization as minimization of the negatives and trust the user to provide the functions pre-conditioned to follow this behavior.

Contributors to the growing function database of Python actively turn new algorithms into codes and furthers into callable functions that are available through the SciPy module [19]. Here SciPy is a collection of tools helpful for scientific application of Python. For ease of usage, there are various distributions of Python that pre package these modules, so users don't have to install them manually. One of the most popular distributions is Anaconda [20]. It includes most scientific tools like NumPy and SciPy and also comes with post processing tools for plotting etc.

Matlab also provides a few optimization routines that are also community supported and has a more user-friendly method with a Graphical User Interface (GUI) to interact with the algorithm and track the functions. Unlike the free-to-use nature of Python, Matlab requires a license and is often less popular among engineers whose primary focus is optimization, because MATLAB offers much more functionality. Thus, using MATLAB for the sole purpose of optimization is not an intelligent application of Matlab. Python allows for selective installation of modules, where as, MATLAB comes as an expensive prepackaged product.

2.10.4 Algorithms

Optimization algorithms in Python include functions that can take different kinds of input. The most appropriate ones will be the ones that include a provision for optimization with constraints. The following are found to have such a provision.

- 1. Conjugate Gradient (CG) algorithm [21] This is a generalization of the Newton CG line search. The linear version of the conjugate gradient algorithm is well understood, but the nonlinear version of this algorithm is surprisingly unpredictable and is not well understood. Thus, this is not a preferred method for nonlinear problems.
- 2. Constrained Optimization BY Linear Approximation (COBYLA) [22] This is an algorithm used in a simplex based optimization program also called COBYLA written by M.J.D Powell. An N-dimensional simplex is constructed, and if a point inside this simplex is found to have a lower value than the vertices, then the nearest vertex is updated with the newly found point thereby making the volume of the simplex smaller with iteration until a satisfactory convergence criterion is met.
- 3. Sequential Large Scale Quadratic Programming (SLSQP) [23] The Sequential Large Scale Quadratic Programming is best suited for problems with a limited number of dimensions, n. The author recommends this algorithm for n<1000. SLSQP requires the least number of iteration for convergence when the function being optimized is continuous. This is also a popular method among engineers at Suzlon because it provides a method to incorporate both constraints and bounds for the parameters.

4. Differential Evolution (DE) [24] - Differential evolution searches for the global minima. It starts with a stochastic and noisy roam through the dimensions of the function and learns its approximate shape. Then starts optimization using gradient descent algorithm from a new starting point, which predicted to be closer to the global minima, it searches for the most optimized solution. This method does not allow for constraints but only takes in a boundary.

The first three of the four above mentioned methods of optimizing are limited to finding the closest local minima inside the bounds. To find the global minima the most popular methods is differential evolution. But this algorithm doesn't incorporate constraints thus to enable constrained optimization of the function one can use a combination of the two. Initially, employ DE to study the bounded region for a few iterations and then choose a suitable starting point inside the bounds to converge towards the global minima while making sure the constraints are respected. This is a recommended method if time allocated for the project is not a limitation.

2.10.5 General performance of the algorithms

A test is devised for understanding the general performance of the said algorithms by providing them with a smooth function of 2, 3, 6 and 12 inputs. These inputs can be thought of as a point in an N-dimensional space. If an N-dimensional space is chosen, then the function is the distance between the input point and [1,1...N times]. Obviously, the minima to this function must lie at exactly [1,1...N times], where the distance becomes zero. The starting point is maintained at [10,10...N times]. The number of times the function has to be evaluated to find the minima is recorded, and the results are presented in Table 2.2.

	No. of iterations for convergence				
Space dimensions $(N) \rightarrow$	2	3	6	12	
COBYLA	43	56	129	320	
CG	20	25	32	56	
$_{ m DE}$	1770	3600	12420	49140	
SLSQP	9	11	17	29	

Table 2.2: Algorithm performance study

Table 2.2 clearly shows for the different N-dimensional spaces provided for the algorithms to work with, DE stands out as the one with the largest number of function evaluations, This is expected behavior for a stochastic algorithm. SLSQP seems to be consistently the fastest and the least sensitive to the magnitude of N.

This study is done with a very focused intent of studying the efficacy of the algorithms at identifying and starting the process of approaching the minima. However, this does not represent an exhaustive study of the algorithms, because this is not the focus of the project.

2.11 Research question

It can be concluded from the literature survey that in order to optimize a joint it is important to study and isolate the factors influencing its performance and cost. The parameters defining a blade root will be numerous, but not all of them will affect the performance equally. It is also necessary to identify the constraints that will be used to guide this optimization process. The process of optimization of mathematical problems are relatively simple when the function and its derivative is known, but while optimizing a large FEM model this could get a lot more complicated and time-consuming thus the process must be streamlined, and the performance of solvers must be considered while choosing the algorithm. Based on the above knowledge the two central research questions and its sub questions can now be framed.

The first set of sub questions will help identify a parameter that can improve the performance of the blade root and also select design parameters which will assist in an efficient manipulation of the design. The blade root must be redesigned but not radically. Thus the parameters that are chosen must help reduce its mass, while, still retaining the basic shape of the blade root. They must not be numerous, owing to convergence difficulties and time constraint.

Q1: What parameters can be used to prepare the blade root design for optimization and the subsequent setting up of the optimizer?

- What is a suitable performance parameter that can be used to study the joint?
- What are the design parameters in the blade root that can be used to manipulate the performance of the joint?
- What are the design parameters in the blade root that can be used to manipulate its mass?

Answers to the above question will lay the groundwork necessary for the optimization process. The parameters chosen will act as manipulators of design in the optimization process and will be treated as inputs into the optimizer. But unless the optimizer has an appropriate property to minimize or optimize, the optimization process will not be meaningful. A subjective definition of optimization will help guide the process. This will depend on what the engineers at Suzlon view as worthy of optimization. It will be helpful to have an insight into the various design constraints that the in-house engineers follow so that the work of the thesis can be useful to the Engineers. Finally, the model used in the thesis is a simplified adaptation of the Suzlon's "Half model" of the blade root. Thus, it must be ensured the design recommendation resulting from the thesis work must bring about similar changes in the Half model as they do in the thesis model. Thus the second central question and its sub questions can be framed. Q2: What are the changes to be made to the current blade root to reduce the effects of local laminate bending on the T-bolt and reduce the overall cost?

- What is an appropriate definition for the degree of optimization and simplification?
- What are the design constraints for the blade root?
- What algorithm can be used to search for the optimized design?
- Does the recommended changes for the optimization of the blade root have the same effects on the performance of Suzlon's Half model of the blade root?

The above question will guide the process of setting up a meaningful optimizer, and subsequent searching for a optimized design. If there exists a set of modifications that can help optimize the blade root as is seen desirable by the design team, then these changes will be tested on the Half model of Suzlon for verification. This will conclude the thesis.

2.12 Conclusion - Literature survey

2.12.1 Optimization - outcome & expectation

The preparation for optimization will focus on identifying parameters that have the highest influence on the performance of the model, and this will enable a more streamlined approach with a lesser number of parameters. The optimization will focus on identifying possible design changes to optimize and simplify the design. Possibilities of reducing the cost of the joint will be investigated, and an appropriate cost function will be setup to enhance the structural optimization. Lessening the number of bolts will also be a favorable outcome and this will either necessitate treating it as a floating point parameter or execute a set of manual function evaluations while reducing the parameter, while treating it as an integer that it is, and monitoring the stresses and fatigue life. The above-mentioned algorithms cannot handle integer parameters and will treat all the inputs as floating point numbers.

2.12.2 Design guidelines

Finally, a set of guide lines will be drawn up alongside a comparison of the optimized design for the blade root with the Reference design, and these guidelines will be verified on the full model at Suzlon. These guidelines will highlight a set of parameters that can be used to improve designs in the future and will also suggest a generalized methodology that can help in the structural optimization process.

Finite element model and optimization framework

In this chapter, the experimental setup used to aid the optimization of the blade root connection will be presented. The details of the finite element model will be discussed followed by the environment used for optimization and its various aspects.

3.1 Software environments and structure of the setup

A finite element model of the blade root is provided by the engineers at Suzlon which has been used and tested for several generations of the blade root design. Convergence studies with respect to the element are assumed to have been done in the past, and it is understood that the engineers at Suzlon have sufficient confidence in the validity of the model.

This model is maintained as a set of Ansys Parametric Design Language (APDL) codes where the parameter definition is kept separate from the instruction set for the various geometric operations to build the blade root. APDL is used, to construct the blade root geometry and analyze it. Stresses from strategic locations identified as most critical are extracted by selecting the nearest node. The post processing of the experimental data is done using an excel spreadsheet prepared by the design engineers at Suzlon. To ensure consistency in the post processing techniques during the thesis work the same spreadsheet is adopted for verification of the codes. The stress data extracted from Ansys is input into the spreadsheet that calculates the performance parameter of the blade root, also called the stress ratio, denoted by Φ . The exact mathematical definition of this parameter is given by Eq. (2.6).

The optimization framework is setup using Python. The same can be done by any programming language that provides inbuilt functions for minimizing functions for which the derivatives are not readily available. Python is chosen as it is the preferred language for programming at Suzlon. It is open source and the community of scientists and engineers working with Python as their primary language has contributed to a very active online database of

function modules and tutorials. Python allows the user to install packages that can add functionality to Python using the PIP Installs Packages (PIP) tool which is provided inbuilt along with most standard distributions of Python. If one is unfamiliar with the intricate structure of Python and its dependencies, there are prepackaged distributions of Python specifically targeted at the engineering and scientific communities. The most popular one is the Anaconda distribution [20]. The most important module used in Python for optimization is SciPy [19], which comes bundled with the Anaconda distribution. SciPy is a collection of scientific function & data libraries, editing tools, data presentation tools and post processing tools.

3.2 Finite element model of the blade root connection

Generally, the blade of a modern day wind turbine that is capable of generating 5MW of power is over 50m long and modeling the entire blade to study the behavior of the blade root is both time and system resource intensive. The engineers at Suzlon use a reduced model of the blade to analyze the stresses at the blade root connection. This model includes the hub bearings (Figure 1.1), the T-bolt assembly embedded in the blade root (Figure 2.2) and 3m of the blade root itself. Only half of the blade is modeled by the engineers in their system because a cylindrical structure subject to bending loads shows symmetric deformation. The plane of symmetry is the axial plane perpendicular to the applied moment. This is a simplification of the model that helps in reducing computation time. A schematic of the blade root model used by Suzlon for its design purpose is shown in Figure 3.1. At the start of the thesis project, the blade root consisted of 88 T-bolts. This finite element model of the blade root consisted of approximately 2 million nodes which is well over the limitations imposed by Ansys for the student license. To adapt the model such that it can be analyzed on a consumer grade laptop with a student license the model is further simplified and this reduced model is also highlighted in Figure 3.1. During the phase of the thesis, the node/element limitation imposed on an Ansys student license was 256000.

3.2.1 Reduced finite element model

Each of the 88 T-bolts in the blade root is placed in a radially symmetric pattern. The reduced model that will be used for the thesis work will model only one bolt and the composite in its vicinity. This bolt will be the one furthest from the axis of moment application and will capture the most critical stress state appearing in the blade root during the worst case scenarios.

3.2.2 Bolt Preload

During the assembly of the blade and hub, the T-bolt is tightened. This tightening induces tension in the shank and compression in the laminate and bearings. The tightening effect can either be modeled by using the pretension element in the T-bolt shank or by using the temperature dependent properties of steel. The T-bolt shank in the FEM model is modeled using the second method with a linear coefficient of thermal expansion, $\alpha = 15 \times 10^{-6}$.

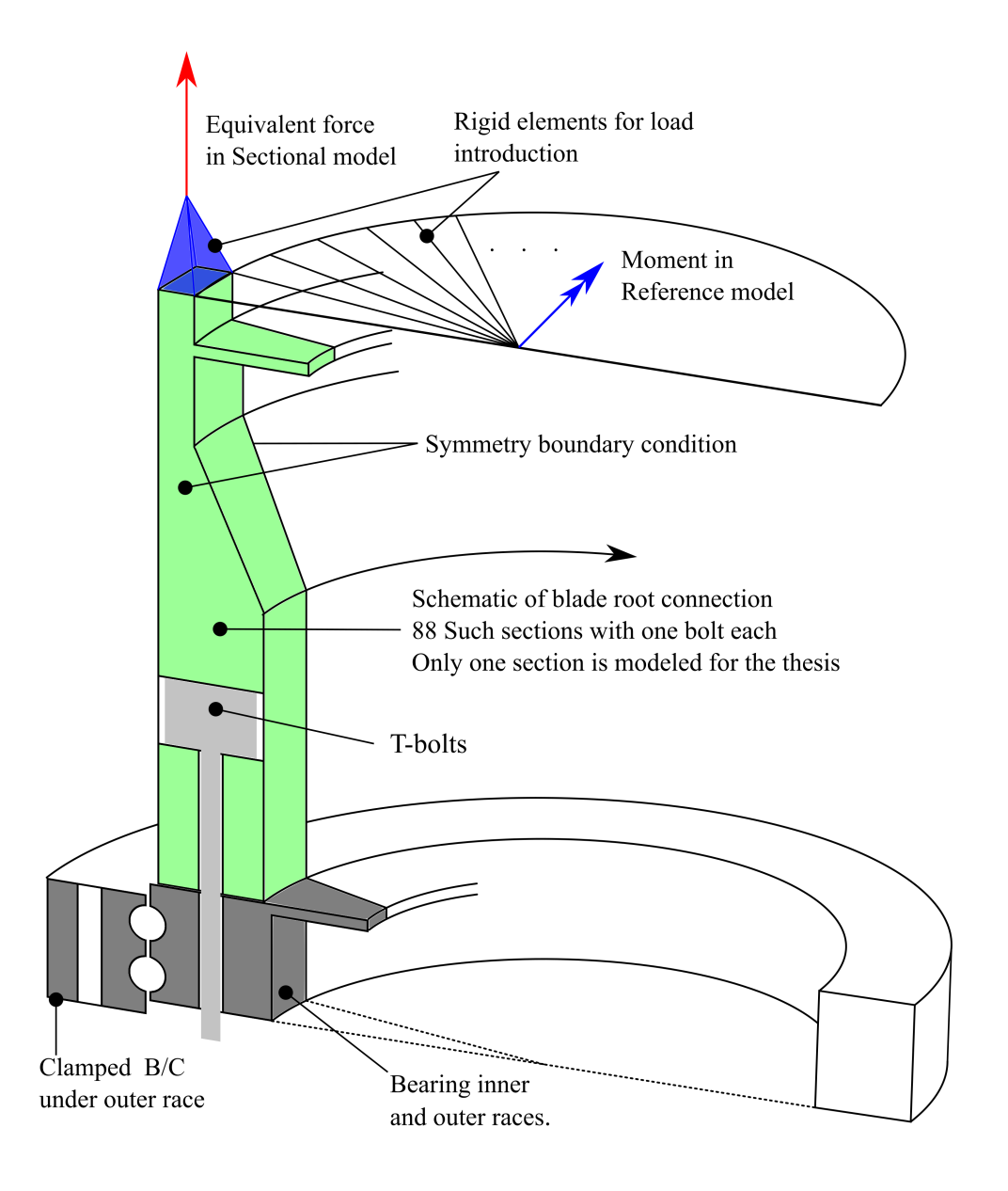


Figure 3.1: Illustration of the features of blade root model

Initially, an arbitrary temperature of $T_{default} = -300^{\circ}C$ is applied to the model, and the stresses are calculated and extracted. The temperature is then linearly scaled depending on the stress in the T-bolt shank to achieve the required prestress in the bolts. The scaling of temperature is carried out using Eq. (3.1). $\sigma_{prestress}$ is the required prestress in the bolt shank. In the Reference design, a value of $\sigma_{prestress} = 540 \text{MPa}$ is used. σ_{bolt} is the stress in the bolt after applying the default temperature. The process takes place in Stage 1 of the central cost function shown in Figure 3.6. T_{bolt} is the temperature that is necessary to produce the required prestress.

$$T_{bolt} = T_{default} \left(\frac{\sigma_{prestress}}{\sigma_{bolt}} \right) \tag{3.1}$$

3.2.3 Load introduction

Subjecting a cylindrical structure like the blade root to a bending moment will produce a continuous axial stress in the shell that varies in a sinusoidal manner along the circumference. This is explained further in Appendix A. But, when reducing the model to just a sector of the blade root, an equivalent force must be applied to the tip of the sector as shown in Figure 3.1. This force represents the overall axial load applied by the stresses in the laminate on the modeled sector alone. A node is created 300mm vertically above the highest point of the blade root model to introduce this load into the laminate. It is rigidly tied to the nearest nodes as shown in Figure 3.2.

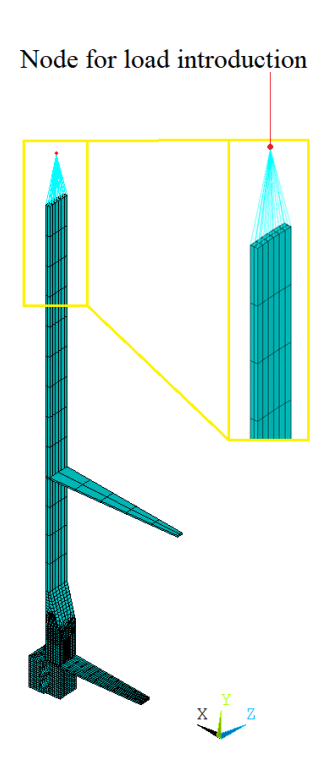


Figure 3.2: Method of introduction of load into the reduced model

The conversion for external moment (M_{ext}) to the force (F_{ext}) on the sector is dictated by Eq. (3.2) which is derived in Appendix A.

$$F_{ext} = M_{ext} \left(\frac{2}{R_{root} N_{bolts}}\right) \sin(\theta_{bolt})$$

$$\theta_{bolt} = 90 - \frac{\theta_{\text{sector}}}{2}$$
(3.2)

 θ_{sector} is the internal angle of the modeled sector of the blade root. θ_{bolt} is the angular position of bolt in blade root, and is illustrated in Figure A.3. These angles depend on the number of

bolts in the blade root. $R_{root} \& N_{bolts}$ are the mean radius of the thick part of the root and the number of bolts respectively.

3.2.4 Boundary conditions

The outer race of the bearing is attached to the hub. As the blade experiences the loads from rotation and wind, all the components in the rotor will experience deformation. But the hub is assumed to be rigid to simplify the model and is not modeled. The bottom surface of the outer race of the bearing is clamped and emulates the presence of the rigid hub. This is shown in Figure 3.3.

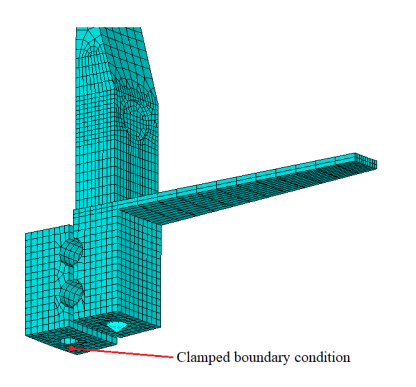


Figure 3.3: Boundary condition at the bearing

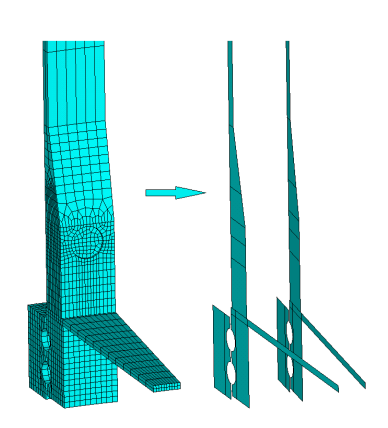


Figure 3.4: Planes of symmetry extracted for clarity

In the Half model, the plane of symmetry along which the blade root has been split into two halves is given the symmetry boundary condition. The Half model is a circular array of the reduced model used for the thesis. Thus, the two radial planes that are shown in Figure 3.4 are given symmetry boundary conditions. These planes lie exactly half way between the modeled T-bolt and its adjacent T-bolts. The boundary conditions are further elucidated in Appendix A. Symmetry boundary condition is chosen over other boundary conditions like axisymmetry and periodic boundary condition because the sole purpose of applying this boundary condition is to reduce the model. Due to the presence of the T-bolt in the center of the laminate asymmetric boundary condition cannot be applied since it assumes the the cross-section of the blade root to be uniform around the axis, which is not the case. The symmetry boundary condition is simplest and most elegant method of reducing the model.

The barrel head is in contact with the surrounding laminate surface. Thus, there is a contact surface defined here. A similar pair of contact surfaces is defined between the composite and the bearing. Both these features of the blade root are sources of nonlinear behavior of the Finite Element Method (FEM) model.

Limitations of boundary conditions

The modeled section lies in a region where the stresses are the highest. The adjacent sections of the blade root lie in areas of lower stresses. This is illustrated in Appendix A. In reality,

the axial stress in the blade root shows a sinusoidal variation along the circumference and in the vicinity of the modeled section the stress variation has a peak. But the symmetry boundary condition mirrors the stress states and deformations in the modeled section onto its neighboring sections. This is a potential cause of differences in behavior between the Half model used by Suzlon and the Sectional model used in this thesis. Similarly, the clamped boundary can also be a source of error when comparing the results from the Half model to the results from the test rig.

3.2.5 Element types in reduced model

To maintain as much similarity as possible between the Sectional model and the Half model the element types are not modified. The elements used in the model are illustrated in figure 3.5.

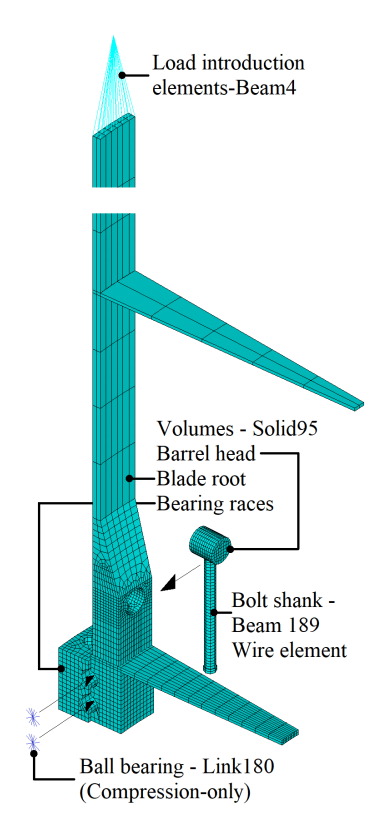


Figure 3.5: Illustration of elements used in the blade root model

All the elements that represent volumes in the model use the *Solid95* element. This element is defined by 20 nodes, with 3 degrees of freedom at each node (translations along X, Y and Z). Assuming a roughly cubical element, the nodes are situated at the 8 corners and the midpoints of the 12 edges. These elements appear in the blade root, the bearing races, and the barrel head. The circular stiffeners in the root and bearing are not treated as separate entities and inherit the same properties as the parts they are attached to.

The ball bearings are modeled as 6 links and meshed using Link180 element. It is a 3D spar element with 2 nodes with 3 degrees of freedom at each node. In this model this element has

stiffness only when in compression. It is a simplified method of modeling the contact between the bearing balls and the raceway.

The T-bolt shank is modeled as a beam with circular cross section. It is meshed with *Beam189* element. It is a quadratic beam element with 6 degrees of freedom at each node (3 for translation and 3 for rotation). This element can output axial, bending and torsional stresses at the nodes which are central to the entire process of optimization. Note that the cross section is only visualized. The shank is actually a wire element.

Beam4 is used for all the rigid constraints used in the model. One such site is the point of load introduction. The highest node shown in Figure 3.2 is tied to the nodes under it with rigid elements with Beam4. Similarly, the shank of the bolt must be attached to the bottom of the bearing. In reality, this is done by the nut. But in the Sectional model, the bottom most node in the T-bolt shank is tied to the bearing using Beam4. This element is made of 2 nodes and has 6 degrees of freedom at each node. This is one of the oldest and simplest beam elements in Ansys.

When the bolt is tightened, the shank of the bolt will experience tension and the bearing along with the surrounding root laminate will undergo compression. This can be modeled using either the pretension element or simply by reducing the temperature of the shank forcing it to contract. The latter is preferred for simplicity. However, there is an additional step to be included in the finite element code. It is convoluted to directly calculate the temperature that must be applied to produce the required pretension. An arbitrary temperature is initially applied, and the stress in the bolt is queried. The temperature is then corrected using Eq. (3.1).

3.3 Material properties

The blade root is made of Glass Fiber Reinforced Plastic (GFRP) laminates. The blade root is subject to both axial and shear loads. The laminate follows a Triax layup. The bearings and the T-bolts are made of steel. In the blade root laminate, material coordinate axis X is parallel to the axis of the blade root. The Y axis is along the circumference, and the Z axis is radial. The material properties are provided in Table 3.1

Property	E_x	E_y	E_z	G_{xy}	G_{yz}	G_{xz}
Steel	210GPa	210GPa	210GPa	81GPa	81GPa	81GPa
GFRP	35.2GPa	14.2GPa	9.94GPa	8.738GPa	4.86GPa	4.86GPa
		Property	μ_{xy}	μ_{yz}	μ_{xz}	
		Steel	0.3	0.3	0.3	-
		GFRP	0.395	0.2	0.2	

Table 3.1: Material properties of Steel and GFRP (Courtesy: Suzlon Energy Ltd.)

3.4 Optimization framework

As mentioned in Section 2.10, the optimization of a structure using its FEM model is a black box optimization. The properties of a design can be extracted by solving the model for the stresses, but it is not practical to predict how the stresses might vary as each of the design parameters are varied. Thus, what we have at hand is a function that accepts the different dimensions of the blade root and in return calculates the stresses in the model for the loads specified. The sensitivity of the stresses to the design parameters is not readily available.

Scipy provides a set of function that can be used as optimizers. These functions are designed to minimize a cost function inside the allowed boundaries while ensuring the constraints are respected. Eq. (2.12) is the mathematical representation of a typical optimization problem. All the constraints identified in the literature survey are converted into callable functions.

The cost function is central to the optimization procedure and sets up the FEM model, post-processes the raw data and records a detailed set of results which will be adequate to recreate the model in the future. The flow chart provided below outlines the various steps in the cost function.

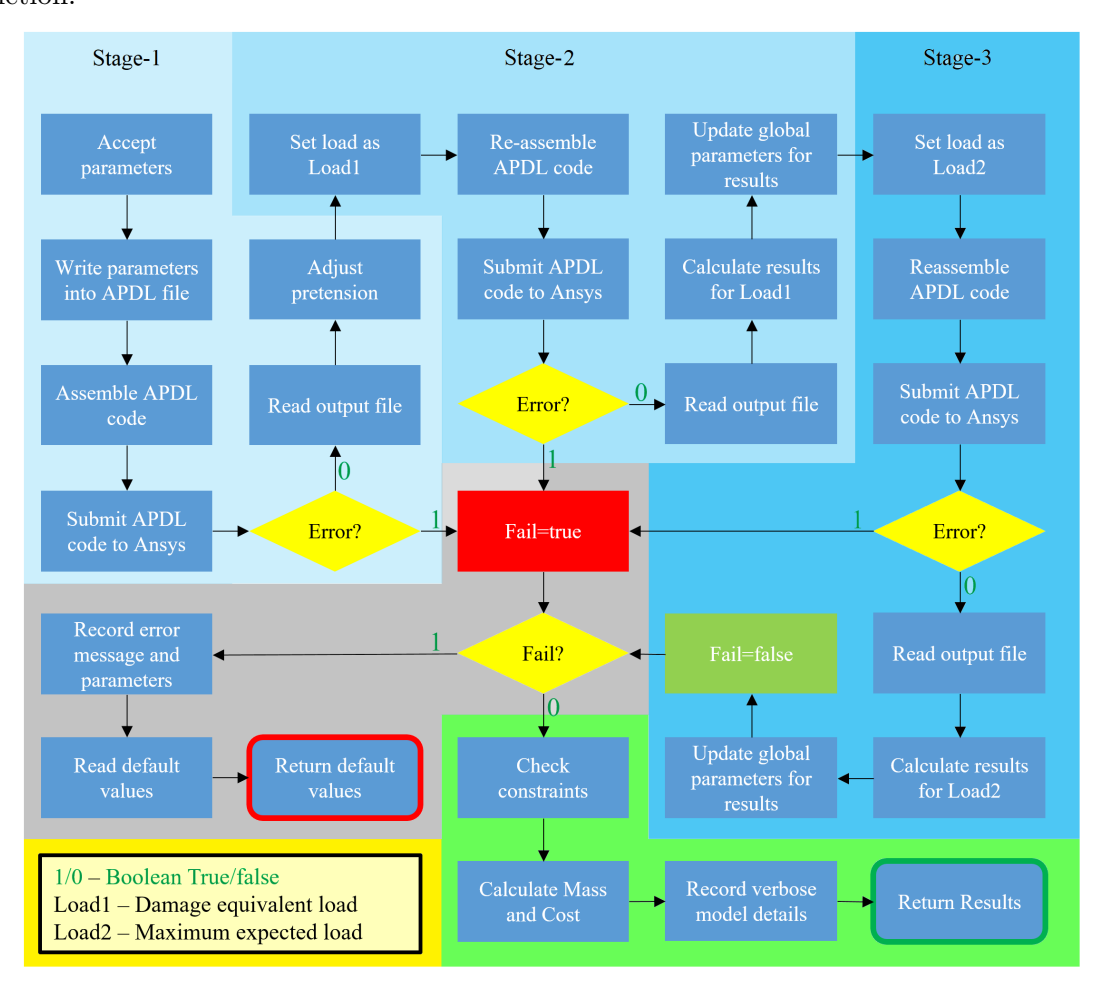


Figure 3.6: Flow chart of the cost function

The logic in the cost function can be broadly classified into three sequential stages. During Stage 1 the cost function is initiated, and it accepts the parameters provided to it, followed by the assembling of the APDL code and its submission to Ansys. Python waits for the processes in Ansys to finish and then post processes the data and adjusts the pretension.

In Stage 2 the focus is on applying the damage equivalent load on the FEM model for fatigue

analysis. The Damage equivalent load is provided by Suzlon as an input and is discussed in Section 2.9.4. The damage equivalent load is applied on the node shown in Figure 3.2, and the stresses are measured, post processed and the data is recorded.

In stage 3 the highest load expected on the blade root is applied. This load is also provided by Suzlon as an input. Similar to Stage 2 the stresses are measured and post processed and recorded. The last check for failure is done to prevent failure of the optimization loop. Any failure is elegantly handled by passing a set of arbitrary default values to avoid the failure of the optimization loop. Various properties of the model are now calculated and stored in global variables. These properties include the mass and cost of each component, the constraint stresses at each load, the temperature for pretension, stress ratio, load, input parameters, performance parameter, the current time stamp, etc. This ensures the model can be recreated in the future if the need arises.

On calling the various callable functions for the constraint stresses the stresses calculated in stage 3 is returned from the global variables. Most of the record keeping is done in text files for easy access. The mass calculation is performed for the modeled region only. The cross sectional area of the blade root and the position of its centroid can be queried from Ansys, and these values are used to calculate the volume of the material used in the root. The T-bolt is treated as a combination of cylinders, and this simplified model is used to calculate its mass and cost. All the information extracted from Ansys is stored in its output file which is specified in the APDL code.

A short summary of the content in the Python frame work is given below and elucidates the various functions in the Python frame work that are setup to aid the optimization process.

- 1. Global registry This is a set of variables accessible globally across all the functions that store the input parameters and results.
- 2. Manipulator function set In Python, the global variable cannot be modified from the editor and can only be accessed from inside a function. This set of functions is used to manipulate the global variables.
- 3. Constraint function set These functions are used to calculate the constraint stresses. They store their results in the global registry.
- 4. The boundary function Some algorithms do not accept the boundaries for the parameters to be varied. One such algorithm is the genetic algorithm, and under such circumstances, the boundaries can be converted to a smooth mathematical function whose value changes from positive to negative when crossing the boundaries. In case the algorithm accepts boundaries explicitly, this function becomes redundant and must be omitted.
- 5. The mass and cost function set The costs of the blade root, bearing and bolts are treated very superficially and is assumed to be a function of only the material costs involved. This is the preferred level of cost calculation at the design department at the stage of optimization and analysis. A higher degree of detail in cost calculation is incorporated at later stages of design and is out of the scope of the thesis.

6. Central fitness function - This function is illustrated in Figure 3.6 and serves the purpose of interfacing Ansys and the optimization algorithms in Python. It also has all the disk input-output functionality. It returns the parameter to be optimized. The cost is seen as the most appropriate aspect for optimization.

3.5 Constraint functions

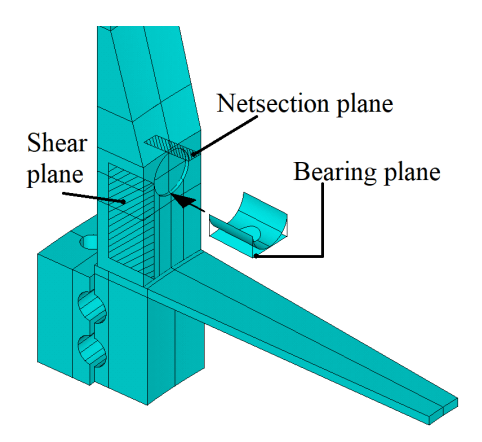


Figure 3.7: Stress planes in the laminate

The constraint stresses are recommended by Suzlon, and the information learned from literature survey agrees with their recommendations. They include the bearing, shear-out, and net-section stresses in the laminate around the T-bolt barrel and the stress in the T-bolt shank. Their ultimate limits are presented in Table 2.1. The laminate stresses appear on distinct planes in the laminate and are illustrated in Figure 3.7 and Figure 2.5. Note that that in Figure 2.5 there are two net-section planes and two shear planes present but only one of each is highlighted in Figure 3.7. The bearing plane is the area of the barrel-head in contact with the laminate projected onto the horizontal plane.

Other constraints include the fatigue life of the bolt. The turbine is designed with a service life of 20 years, and the optimization process attempts to limit the fatigue life as close to 20 years as possible. A design optimized for minimum stresses will have excess fatigue life and high cost. This is undesirable. Thus, minimum material cost and complexity of design is desired while maintaining 20 years fatigue life. The method for fatigue analysis is presented at a later stage in the report.

3.5.1 Bearing failure

The first mode of failure is the bearing failure under the barrel head. The stress appearing on the bearing plane, as a result of the combination of pretension in the T-bolt and external loading, must be maintained below the ultimate crushing strength of the laminate. The ultimate limit recommended for this stress is 220MPa with a safety factor of 2.2. this gives a design limit for the bearing stress as 99.5MPa.

At maximum expected load on the blade root, the force generated by the bearing stress is the reaction to the force applied by the bolt shank on the barrelhead. These forces must be equal and opposite. Thus, the stress of the bolt shank is queried from the model of the blade root and is converted into bearing stress using Eq. (3.3).

$$\sigma_{\text{bearing}} = \frac{\sigma_{\text{bolt}} \left(A_{\text{bolt}} \right)}{A_{\text{bearing}}}$$
 (3.3)

To incorporate it into the bearing stress constraint function the difference between the design limit and the bearing stress is calculated. Thus, the bearing stress constraint function ensures $99.5 \text{MPa} - \sigma_{\text{bearing}} > 0$.

3.5.2 Shear-out failure

The second mode of failure is the shear out of the barrel head due to excessive shear stress in the laminate. Shear stress is assumed to be zero after pretension and is contributed to only by the external loading. The ultimate limit for shear stress in the laminate is recommended by the design team as 200MPa with a safety factor of 2.2. This gives a maximum design limit of 90MPa.

When the blade experiences maximum load, the force applied at the tip side of the root will bypass the barrel head and enter the laminate under it via the net section planes and subsequently the shear planes. Thus at the maximum expected load, the force applied to the blade root Sectional model is converted to the stress on the shear plane using Eq. (3.4).

$$\sigma_{\text{shearing}} = \frac{F_{\text{ext}}}{A_{\text{shearing}}} \tag{3.4}$$

Note that $A_{\rm shearing}$ is the total area resisting the external load and is twice the area shown in Figure 3.7. This is incorporated into the Shear-out failure constraint by calculating the difference between the design limit and shear stress. Thus the shear-out failure constraint function ensures $90{\rm MPa} - \sigma_{\rm shearing} > 0$.

3.5.3 Net-section failure

The third mode of failure to be checked for is the Net-section failure. The externally applied load is the only contributor to the net-section stress and the maximum expected load on the blade root is converted to the net-section stress using Eq. (3.5).

$$\sigma_{\text{net-section}} = \frac{F_{\text{ext}}}{A_{\text{net-section}}}$$
 (3.5)

Note that the $A_{\rm net-section}$ is the total net section area in the Sectional model of the blade root and is twice the area shown in Figure 3.7. The design team recommends an ultimate limit for the net-section stress, which is the tensile limit for the laminate, as 480MPa with a safety factor of 2.2. This gives a design limit of 217.2MPa. To incorporate it into the set of constraints the difference between the design limit and the stress is calculated. Thus the net-section failure constraint function ensures 217.2MPa – $\sigma_{\rm net-section} > 0$.

3.5.4 Tensile failure of the T-bolt shank

The stresses in the T-bolt shank are a contribution of the axial, bending and torsion loads. Tightening of the T-bolts during installation of the blade root contributes to the torsion and axial loads and during the external loading these stresses are exacerbated by additional axial and bending loads. After applying the maximum expected load on the model, the axial and bending stresses in the bolt are extracted from preset points near the barrel and near the bearing. The loads are illustrated in Figure 2.12.

Von Mises failure criterion is recommended for the bolt failure constraint. The maximum tensile stress combined with the torsional stress is check for failure using Eq. (3.6).

$$\frac{\sigma_{\text{yeild}}}{1.1} > \sqrt{(\sigma_{\text{ax_total}})^2 + \tau^2}$$
(3.6)

This equation is elucidated in section 2.9.2 where the relation for the shear stress due to bolt tighten torque τ is presented. $\sigma_{\rm yeild}$ is taken as 900MPa with a safety factor of 1.1. The design limit of the Von Mises stress in the bolt is 818.2MPa Thus the bolt failure constraint function ensures 818.2MPa $-\sqrt{(\sigma_{\rm ax_total})^2 + \tau^2} > 0$.

3.5.5 Fatigue life constraint

Through out the life of the wind turbine, it is subject to a load spectrum that includes calm days with steady wind and occasional strong winds and other rare cases of bird hits or severe storms. The loading a blade under goes is recorded and analyzed, and the Markov's matrix is provided by Suzlon along with the damage equivalent load. Markov's matrix is the result of the rain flow counting technique applied on the time history of the loads on the blade root. The damage equivalent load is the amplitude of the alternating load that, in theory, produces the same damage as the unprocessed loads.

During the preliminary stages of the thesis work, the damage equivalent load method is adopted. The stresses appearing in the bolts of the reference design on the application of the damage equivalent load is noted as the limit stress (σ_{DaEq}). During the optimization process, it is ensured that total axial stress in the bolt ($\sigma_{\text{ax_total}}$) does not cross this limit when applying damage equivalent load. The damage equivalent stress limit is provided in Table 2.1. In the final stages of the design optimization, the recommendations are adopted into the Half model, and the various stress ratios at different loads are extracted. Then the Markov's matrix is used to find the stresses in the bolts for each loading amplitude, and a detailed fatigue study is conducted, and in the case of fatigue failure, the design is manually modified to pass the constraints.

To incorporate the fatigue life constraint into the optimizer Eq. (3.7) is used. This stress check is done only at the prescribed damage equivalent load of 3MNm.

$$\sigma_{\text{DaEq}} > \sigma_{\text{ax total}}$$
 (3.7)

The fatigue life constraint function ensures $24\text{MPa}-\sigma_{\text{ax_total}}>0$. σ_{DaEq} can be found in Table 2.1.

3.6 Optimization algorithms

Sequential Quadratic Programming (SQP) or the Sequential Large Scale Quadratic Programming (SLSQP) algorithm is the fastest algorithm to minimize the function if an appropriate starting point is provided. This algorithm is often the recommended algorithm by the developers of packages like fmincon of MATLAB and Scipy. It is the most robust and efficient technique for black box optimization. It is also the preferred algorithm at Suzlon because the boundaries for the parameters can be explicitly inputted into the optimizer and need not be treated as a function. SQP and SLSQP are essentially one and the same. Different software packages refer to the Sequential Quadratic Programming algorithm with different names. In Python, the algorithm can be applied to problems with a very large number of parameters and constraints functions and, thus, it is referred to as Sequential Large Scale Quadratic Programming (SLSQP).

SQP, much like most other algorithms, treats the parameters as a point in an N-dimensional space. A design can be visualized as a point in the N-dimensional space with the output values imagined as the properties of that point. Each design parameter being varied lies on one of the axes of the space. Thus the reference design provided by Suzlon lies somewhere in this space. But it is impossible to predict what the nature of variation of the properties will be as the design is modified. This is a direct implication of the problem being a black box problem.

One of the major drawbacks of the algorithms bundled in the SciPy module is that they treat all the parameters as floats. This is acceptable if the parameter being modified is a length. But features of the blade root like the number of bolts cannot be treated as floating point numbers in reality. So it is, in theory, possible to treat the number of bolts as a floating point number because the number of bolts only determines what the internal angle of the modeled sector will be. Thus, at a later stage they must be converted to the nearest feasible integer so that the changes can be translated to Suzlon's Half model of the blade root.

All the above algorithms are available in Scipy through the *Minimize* sub-module. This sub-module which is part of the Scipy package contains the various functions that can minimize other functions. The most popular minimization function is minimize() that can minimize other function using a range of algorithms like SQP (section 2.10.4). A typical minimization function call is provided below.

$$R = \text{minimize}(A, x_0, \text{method} = \text{`SLSQP'}, \text{bounds} = B, \text{constraints} = C)$$

The function being minimized is 'A', starting from an initial point of ' x_0 ,' using the "SLSQP" algorithm. The function is constrained inside the bounds defined in 'B' as the upper bound, and lower bound for each parameter, and the constraint functions in 'C' must be maintained positive. In the blade root, the constraint stresses have design limits. So the difference between the design limit stresses and the stresses appearing in the system must be positive. $\sigma_{design} - \sigma > 0$ where σ is the stress queried from the finite element model of the blade root.

Optimization

In this chapter, the methodology followed to optimize the design of the blade root is described along with the motivation and ideology behind the method. Initially, the formulation of the constraint functions is described followed by a discussion on the cost function for optimization. Then a set of parameters is identified that can help in manipulating the design of the blade root. The parameters are categorized based on the property of the blade root they can effectively modify. The definition of the constraint function contributes significantly to this judgment. The chapter is concluded after presenting an abstraction of the optimization process or a philosophy of optimization that can help in the optimization of the future designs.

4.1 General ideology behind the optimization procedure

The mathematical operations like calculating the Jacobian of the objective function is not discussed, but a superficial understanding of the behavior of the algorithm can help in setting it up and understanding the different kinds of convergence criteria. An optimizer works best when the starting point is both feasible and well within the boundaries of the problem. Starting the optimizer from a point on the boundary may lead to premature convergence to a point which is not adequately optimized.

Since the problem is a black box function, the optimizer does not have any information on its slope and will increment each parameter by a preset value to measure the partial derivatives. These local steps must not disrespect the boundaries and constraints. It is observed that a more optimized result is obtained when there is a larger margin between the constraint values and their limits.

4.1.1 Optimization and convergence

The initial point, boundaries, and list of constraints are passed as arguments along with a cost function that must be minimized while initializing the optimizer. A gradient descent

38 Optimization

optimizer, like SQP, will first study the function in the vicinity of the initial point by incrementing the parameters one by one and evaluating the function at those points. This study will provide the optimizer with the direction of highest descent. Subsequently, it will move in this direction for a preset distance before studying the new point and repeating the procedure until convergence is detected.

If the optimizer is following a stochastic algorithm, then the intent is to find the global minima inside the boundaries provided. The procedure starts by evaluating the function inside the boundaries at randomly chosen points such that all of the space inside the boundary is examined. Then the movement of the optimizer is restricted to smaller and smaller areas that shrink around the approximate location of the global minima. Since this is a stochastic procedure, it is not recommended for problems with a large number of parameters or for problems that take too long to be evaluated. A nonlinear Finite Element Method (FEM) model might take a duration ranging from several minutes to a few hours to converge depending on the model complexity and system specifications. Under such circumstances, it is best to adopt a gradient descent algorithm.

4.1.2 Convergence

The procedure of searching for the minima and moving towards it is repeated until criteria for convergence is met. Convergence could be declared if a minimum is reached, a boundary is approached or if one of the constraint functions becomes critical. If a boundary is approached, then the movement is restricted, and the step size between two designs progressively reduces. This is undesirable in the early stages of the optimization. This kind of convergence might be inevitable if the cost function is monotonically decreasing. If a constraint function becomes critical, the optimizer will attempt to trace back its steps and find the closest feasible point and declares convergence. Here, the desirable and practically useful form of convergence is if minimum is reached. Approaching the boundary or the constraint functions becoming critical at the early stages of the optimization will force the optimizer to stop before any useful reduction in cost is seen. But this form of convergence may be acceptable if a substantial cost reduction is found.

4.1.3 Ideology

The ideology followed is an abstraction of all the subjective inferences of testing and examining the behavior of the optimizer throughout the thesis phase. To ensure convergence to a minimum inside the boundaries of the problem the blade root must be first over designed such that none of the constraints are critical. The designs at Suzlon are often optimized for the fatigue life. Thus it is recommended that the stresses in the bolt be reduced before the initiation of the optimizer. Only then the optimizer must be initiated to reduce the overall cost of the blade root.

It is expected that during the process of optimization the constraint functions will become increasingly critical, especially the bearing stress and bolt stress. This is mitigated by stopping the optimizer and manually increasing barrel head radius and bolt shank radius in the Ansys Parametric Design Language (APDL) code before restarting the optimizer from the latest design.

This is not a standard method but a method that provided the most substantial and reliable results. Optimization algorithms that interface with FEM software tend to be very demanding on resource and time. Plugging in all the conceivable parameters into an optimizer may provide results eventually but it is very slow, and due to the time constraints automation and manual manipulation are combined to get faster results.

4.2 Stress ratio and joint behavior

The joint behavior is initially studied using the stress ratio. This parameter is explained in Section 2.8.2. The stress-ratio is the fraction of the external load that appears on the bolt. Because of the presence of the bearing that induces local bending loads in the laminate and bolts the behavior of the stress ratio is quite nonlinear. The behavior of the stress ratio is studied at bending loads of 2MNm, 3MNm, 4MNm, 6MNm, 9MNm & 10.5MNm. But to streamline the process of optimization stress values only at 3MNm and 10.5MNm are extracted. 3MNm is the damage equivalent load, and 10.5MNm is the highest expected bending moment on the blade root. The joint opening is expected in the blade root only at very high loads close to 10.5MNm and generally above 6MNm.

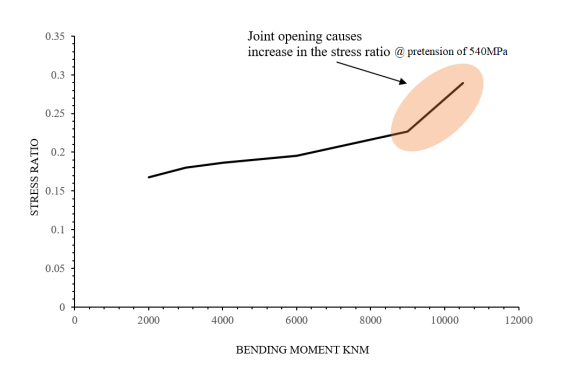


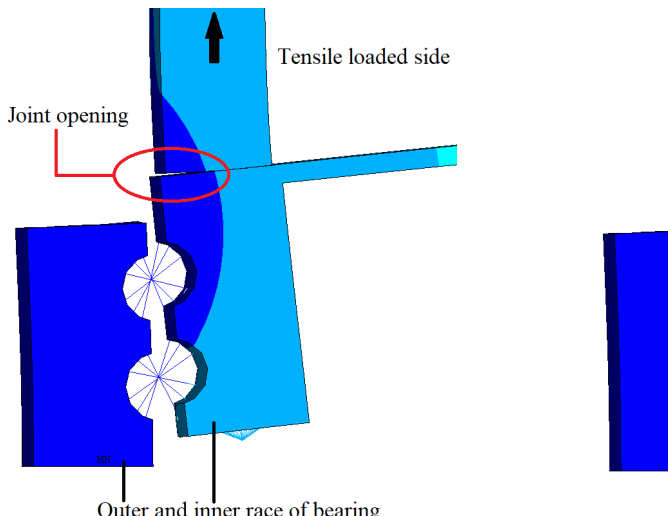
Figure 4.1: Stress ratio increase in reference design during joint opening

Figure 4.2: Stress ratio after increasing pretension in the bolt

The extent of joint opening must first be minimized to optimize the joint and progressively increasing the bolt pretension from the reference value of 540MPa to 640MPa showed a satisfactory reduction in the joint opening. This is reflected in a much more flat stress ratio curve as seen in Figure 4.1 and Figure 4.2. The reduction in the joint opening is also apparent in Figure 4.3 & Figure 4.4. To make the joint opening visible a scale factor of 20 is used while plotting the displacement vector sum in Ansys APDL.

The Reference design at Suzlon uses a pretension of 540MPa, and a modified value of 640 MPa is recommended to reduce the extent of joint opening. As the joint gradually opens from the outer periphery of the blade root as shown in Figure 4.3, the contact area between the composite and the bearing reduces increasing the risk of crushing of the laminate. This also drastically increases the stresses in the bolt and can make the bolt stress increasingly more critical. With an increased pretension a much higher load is required to produce joint opening comparable to the joint opening at 10.5MNm with a pretension of 540MPa.

40 Optimization





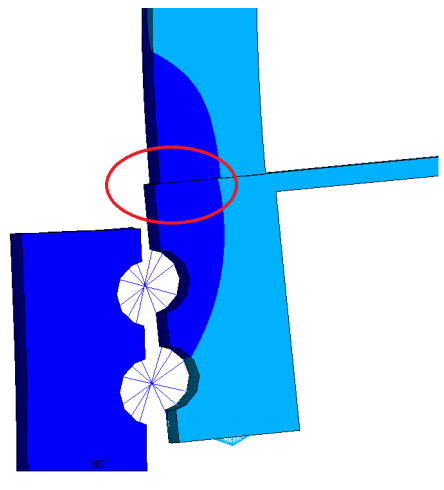


Figure 4.4: Prestress - 640MPa

4.3 Parameter identification

As a general rule of thumb, it can be inferred from Table 2.2 that on increasing the number of parameters defining a problem the number of iterations required to optimize the problem increases. Thus, critical design parameters are chosen to be input into the optimizer so that convergence to an optimized solution can be expected in the limited time frame available.

4.3.1 **Cost function parameters**

The material cost of the blade root is a direct function of the volume of the blade root and bolts combined. Thus the defining dimensions of the blade root cross section and the number of bolts are the prime candidates for the optimization parameters. The dimensions of the bearings are not modified so that most of the modifications can be isolated to parameters controlled by Suzlon. The following parameters are illustrated in Figure 4.5.

- 1. The blade root inner radius (Ri)
- 2. The length of the thick part of the blade root (L1)
- 3. The length of the transition part of the blade root (L2)
- 4. The number of bolts in the blade root (Nb)

These are the parameters which will be manipulated by the cost function. The outer diameter and the thickness of the thin part of the blade root are not modified because this will affect the rest of the blade root.

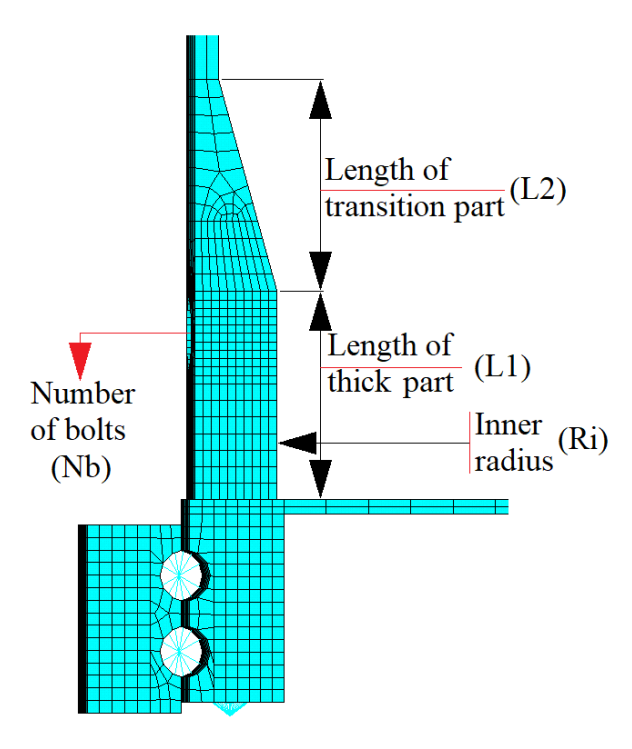


Figure 4.5: Blade root optimization parameters

4.3.2 Constraint parameters

Optimization algorithms always work best when the design they are attempting to optimize has a considerable margin in their constraint function before which the design becomes infeasible. It must be ensured that the stresses are all well below their design limits. As it can be seen from the constraint function description, each constraint stress is a function of a certain area. Increasing these areas will reduce their corresponding stresses and will push the stresses in the model further away from their design limits.

The bearing stress can be controlled by increasing the bearing area which is a function of the root thickness and the barrel diameter as seen in Figure 3.7. The net section area is a function of the distance between the barrels and the root thickness. Reducing the number of bolts will increase the distance between the two bolts and will increase the net-section area. Increasing the root laminate thickness will have a similar influence. The shear area is again a function of the root laminate thickness and the distance between the barrel head and the bearing. The bolt stress is a function of the bolt area alone and increasing the bolt area will push the bolt stress away from its limit stress. The bolt stress is checked at damage equivalent load, and the maximum expected load, and it is ensured the stresses are below the corresponding limits. In Table 4.1, only the Bolt fatigue stress at the damage equivalent load is presented. The values for the constraint stresses in the Reference design is presented in Table 4.1.

42 Optimization

	Stress	Limit	Margin
	(MPa)	(MPa)	(MPa)
Bearing stress	68.8	90.5	21.7
Net-section stress	93.8	217.2	123.4
Shear stress	5.8	90.5	84.7
Bolt fatigue stress	22	28	6

Table 4.1: Initial constraint stress values and their limits

4.4 Initial over design of the blade root and its implications

As a preparation for the optimization process, the blade root is first over-designed. This process involves manipulating key features of the blade root aimed at reducing the constraint stresses below their design limits.

The following modifications are carried out.

- 1. The pretension is increased from 540MPa to 640MPa as described in Section 4.2. This helps in reducing the joint opening. It must be noted that increasing the pretension to values close to the yield stress of the bolt material will drastically affect the fatigue life of the blade root.
- 2. The bolt radius is increased from 28mm to 30mm. This reduces the bolt stress. The bolt radius is restricted by the 39mm diameter hole drilled in the laminate and bearing for the bolt shank.
- 3. The blade root thickness is increased from 100mm to 110mm. This has an influence on all the laminate constraint stresses and helps reduce them. It is ensured that the inner radius of the blade root is greater than the inner radius of the bearing. It is not desirable for the blade root laminate to overlap with the bearing stiffener. Increasing the root laminate thickness results in an increase in the lengthening of the T-bolt barrel head. The barrel length is constrained to be 5mm lesser than the root laminate thickness. This is a thumb rule followed at Suzlon.
- 4. The barrel head radius is increased from 60mm to 65mm. This compliments the reduction of the bearing stress. It is ensured that the increase in the barrel head diameter does not reduce the net section area such that it causes net section stresses to become critical.

The mass and cost of the blade root before and after the modifications mentioned above are contrasted in Table 4.2. The rates used for calculating the cost of the blade root are the most probable rates for the material which are the standard market costs. They do not represent the actual rates of the material which is not disclosed to respect the privacy restrictions.

These modifications to the blade root reduce the constraint stresses and the stresses are tabulated in Table 4.3. It can be seen that the critical stresses are lesser than the stresses presented in Table 4.1. Net section stress is higher after the modification but is still not nearly as critical as the bearing stress.

	Referen	Reference design		n Initial overdesign	
Components	Mass (Kg)	Cost (Euro)	Mass (Kg)	Cost (Euro)	Rate (Euro/Kg)
Blade root	1565	4695.6	1593	4779	3
Bolts	308	1846.8	378	2268	6
Total	1873	6542	2070	7047	

Table 4.2: Mass and cost comparison (Reference vs over design)

	Stress	Limit	Margin
	(MPa)	(MPa)	(MPa)
Bearing stress	64.7	90.5	25.8
Net-section stress	113.03	217.2	104.17
Shear stress	5.27	90.5	85.23
Bolt fatigue stress	15.93	24	8.07

Table 4.3: Constraint stresses after initial over design

This initial over-design of the blade root was necessitated because the reference design of the blade root was optimized for fatigue life of the T-bolt by the design team of Suzlon. Thus any mass or cost optimization attempt exacerbated the bolt stress which was constrained to be lower than the bolt stress in the reference model at the damage equivalent bending load of 3MNm. Such a stress state in the bolt combined with the convergence behavior elucidated in section 4.1.2 caused premature convergence of the optimizer without any considerable design modification to the blade root. These failed procedures are not detailed further as they did not contribute to the optimization process.

4.5 Optimization of the blade root connection

After the initial redesign, the blade root is both heavier and costlier than the Reference design because every modification has resulted in an increase in the mass. In this phase of optimization, the focus is set on reducing the cost of the blade. The resulting design of this process of optimization will be referred to as the *Optimized design*.

The Minimize() function from Scipy module in Python is called. The algorithm employed is the Sequential Large Scale Quadratic Programming (SLSQP) which among all the available optimization algorithms in Scipy showed the fastest convergence to a solution for the test problem detailed in Section 2.10.5. For a well behaved smooth problem with up-to 5 parameters, the SLSQP algorithm is expected to take less than 20 steps for convergence. But due to the inherent non-linearity in the FEM model owing to contacts and joint opening the optimizer is allowed to run for at least 100 iteration before examining the solution. The upper and lower boundaries for the optimization parameters are given in Table 4.4

Due to time constraints, the optimizer is initiated 3 times, and the phase between an initiation and convergence is called the *Optimization Round*. The first time the Reference design with the over design modifications is used as the input design. After the optimizer converges, the barrel head diameter and the bolt shank diameter are manually increased in the APDL code, and the optimizer is restarted with the latest modified design as the starting design.

44 Optimization

	Ri (mm)	L1 (mm)	L2 (mm)	Nb
Upper bound	1170	700	400	90
Initial point	1150	217	285	88
Lower bound	1110	200	100	40

Table 4.4: Optimization parameters and their boundaries

The event of the Round convergence is referred to as a Stage. The barrel head diameter (Bhd) sees a change from 60mm in the reference design to 80mm in Stage III, but this 20mm increase has been carried out in 3 steps. If this modification was done all at once in the initial over design, the net section failure would have prevented any further optimization. As the optimization progresses the number of bolts gradually reduce and the bolts can get larger with bigger barrel heads and bolt shanks. The bolt shank diameter (Bd) is increased from 28mm in the reference design to 32mm in Stage III. The Stage III design is also referred to as the $Optimized\ design$. The Reference design and the $Optimized\ design$ are compared in Table 4.5 and Table 4.6, respectively.

Reference Design					
Ri (mm)	1150	Blade mass -	1565	Kg	
L1 (mm)	217	GFRP rate -	3	Euros/Kg	
L2 (mm)	285	Blade cost -	4696	Euros	
Bd (mm)	28	Bolts mass -	308	Kg	
Bhd (mm)	60	Steel rate -	6	Euros/Kg	
Nb	88	Bolt cost -	1847	Euros	
Representative fraction		Total cost -	6543	Euros	
6543/6543	= 1				

Table 4.5: Dimensions and properties of Reference design

Optimized Design					
Ri (mm)	1160	Blademass -	1497	Kg	
L1 (mm)	225	GFRP rate -	3	Euros/Kg	
L2 (mm)	230	Blade cost -	4490	Euros	
Bd (mm)	32	Bolt mass -	265	Kg	
Bhd (mm)	80	Steel rate -	6	Euros/Kg	
Nb	52	Bolt cost -	1593	Euros	
Representative fraction		Total cost -	6083	Euros	
6083/6543	= 0.93	Cost saving -	460	Euros	

Table 4.6: Dimensions and properties of Optimized design 1

Since the costs of components are calculated using the standard rates of the market, it is more appropriate to view to relative cost variation of the model. This is indicated by the *Representative fraction* of the cost. This quantity indicates what fraction of the initial cost is the cost of the Optimized design. A *Representative fraction* value of 1 represents the Reference design, and this value must be as far below 1 as possible for an Optimized design. The attempt at optimizing the blade root has brought the *Representative fraction* down from

1 to .93. This indicates a reduction in the model cost by 7%.

The Optimized design of the blade root has a root laminate that is 10mm thinner than the reference design. The Reference design has a root laminate thickness of 100mm. This 10mm reduction is possible due to a decrease in the number of bolts from 88 to 52 in the Optimized design. The decrease in the number of bolts is supported by the larger barrel diameter and the larger bolt shank radius. A detailed illustration of the blade root is provided in Appendix B.

The stresses in the *Optimized design* are presented in Table 4.7. The optimized design shows a reduction in the bolt stress at the damage equivalent load. This is very important because the bolt prestress is now higher. At higher prestress values the allowable alternating damage equivalent load is lower. This effect is often captured by the Goodman and Gerber diagrams of mean and alternating stresses for constant life. The convergence is assumed to have been declared due to the bolt fatigue stress becoming critical. This is not a conclusive fatigue analysis of the joint and a more advanced fatigue model using the load spectrum acquired from Suzlon is discussed in Section 4.7.

	Stress	Limit	Margin
	(MPa)	(MPa)	(MPa)
Bearing stress	78.43	90.5	12.07
Net-section stress	65.12	217.2	152.08
Shear stress	10.78	90.5	79.72
Bolt fatigue stress	23.8	24	.2
Bolt max stress	744.00	818.2	74.2

Table 4.7: Constraint stresses in optimized design

4.6 Stages of optimization

Achieving the Optimized design was a 3 stage process where the optimizer was interrupted after sets of 80, 90, and 130 iterations, and the parameters Bhd and Bd were incremented. A considerable amount of drop in cost was observed before the interruption. The intermediate models are not detailed. The barrel head and bolt shank diameter along with the resulting number of bolts at the end of each stage are given in Table 4.8.

	Bhd	Bd	Nb
	$_{ m mm}$	mm	[-]
Initial	60	28	88
Stage I	65	30	80
Stage II	80	32	68
Stage III	80	32	52

Table 4.8: Bhd and Br at the three stages of optimization

Figure 4.6 illustrates the convergence of the optimizer. The entire process is 300 iterations at the Stage III design. The Round 1 of optimization converges after 80 iterations. The

46 Optimization

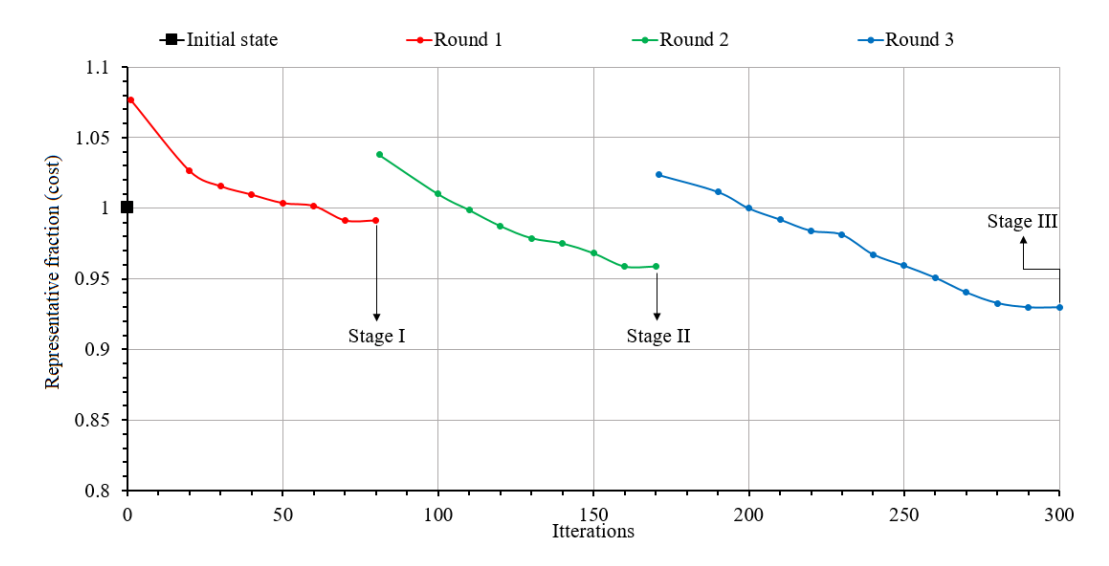


Figure 4.6: Convergence of optimizer

optimizer is interrupted, and the APDL code is modified by increasing the Bhd and Bd values as mentioned in Table 4.8. Then the optimizer is restarted from the latest set of parameters.

The Round 2 of optimization converges after an additional 90 iterations at the Stage II design. The optimizer is duly interrupted and the Stage 2 increments from Table 4.8 is applied to the APDL code. Then the optimizer is restarted again.

The Round 3 of optimization converged after an additional 130 iterations. This is the Stage III design or the Optimized design. The optimizer iterations, convergence and interruptions are shown in Figure 4.6.

4.7 Fatigue analysis of the T-bolts

During the optimization, a simplified fatigue calculation was adopted for the T-bolt. But after the cost optimization, the Markov's matrix is used to ensure the stresses in the bolts do not cause fatigue failure. The time data of all the loads experienced by the blade root is processed to obtain a data set that contains the mean & range and the number of occurrences of the bending moments. Thus, the idea is to convert the seemingly random time data of the bending moments on the blade root to an orderly set of sinusoidal excitation of different magnitudes and occurrences that cause the same damage as the time data. This is done by rain-flow counting. The procedure of rain-flow counting is out of the scope of the thesis and the post processed data set is provided as an input by the design team of Suzlon. This data set will be referred to as the load spectrum.

The fatigue analysis of the T-bolts is best carried out on the Half model. The reason for carrying out the fatigue analysis in the Half model is explained in Section 4.7.2. The design modifications are applied to the Half model. And the stresses and stress ratios at the loads mentioned in Section 4.2 are extracted. The following procedure is followed for the fatigue analysis of the optimized design of blade root.

- 1. The mean bending moments and corresponding ranges are converted to maximum and minimum bending moments on the blade root. $M_{Max}=M_{Mean}+M_{Range}/2$ & $M_{Min}=M_{Mean}-M_{Range}/2$.
- 2. The M_{Max} and M_{Min} are converted to the corresponding loads P_{Max} and P_{Min} using equation Eq. (3.2). P is the external load appearing on the joint and the loads are further converted to stresses. But only a fraction of the external load P_{Max} and P_{Min} appears on the bolts, and this fraction is represented by the stress ratio.
- 3. The corresponding stress ratio for the M_{Max} and M_{Min} are interpolated from the stress ratio data extracted from the Half model, and the loads are converted to stresses in the bolts using Eq. (2.6).
- 4. The stress in the bolt for the P_{Max} and P_{Min} is converted to the mean and range, σ_{Mean} and σ_{Range} .
- 5. The SN line provided by Det Norske Veritas (DNV) Germanischer Lloyd (GL) (2010) [18] is used to extract the allowable number of loading cycles for each stress range in the load spectrum. The SN curve is dependent on the prestress in the bolt, and thus the mean stresses can be ignored as they are accounted for in the SN curve. This SN line for a pretension of 640MPa is presented in Figure 4.7.
- 6. The Miner's rules is then followed to find the fatigue damage caused by the load spectrum. This damage value must be lesser than 1, and the miner's rule is mathematically represented in Eq. (4.1). Here n is the total number of mean-range pairs in the load spectrum, N_i is the number of occurrence of the i^{th} load and $N_{i-allowable}$ is the allowable number of cycles for the i^{th} load from the SN curve.

$$\sum_{i=1}^{n} \left(\frac{N_i}{N_{i-allowable}} \right) < 1 \tag{4.1}$$

4.7.1 SN Curve

The SN curve defined by DNV GL is constituted of two lines that intersect at a point with $N_{allowable} = 5 \times 10^6$. The σ_{Range} at this intersection point is called the detail category of the curve. If this point is known, then the SN curve can be constructed. Below $N_{allowable} = 5 \times 10^6$, the SN curve plotted on a log-log scale has a slope of -(1/3) called the m=3 curve, and above it, the curve has a slope of -(1/5) and is called the m=5 curve.

The detail category of the SN curve is determined by Eq. (4.2) and is limited to a maximum of 85 for bolts smaller than M30.

Detail category =
$$71 \left(2 - \frac{\sigma_{\text{bolt max}}}{\sigma_{yeild}} \right) < 85$$

$$k_s = \left(\frac{30}{d} \right)^{0.25}$$
(4.2)

48 Optimization

 $\sigma_{\rm bolt\ max}$ is the maximum expected stresses in the bolt shank and it is calculated by applying the maximum expected load on the blade root. σ_{yeild} is 900MPa for steel. For bolts larger then M30 a reduction factor of k_s must be applied to the detail category. The SN line, constructed for a bolt with 640MPa as pretension stress, used for the fatigue analysis of the Optimized design is presented in Figure 4.7.

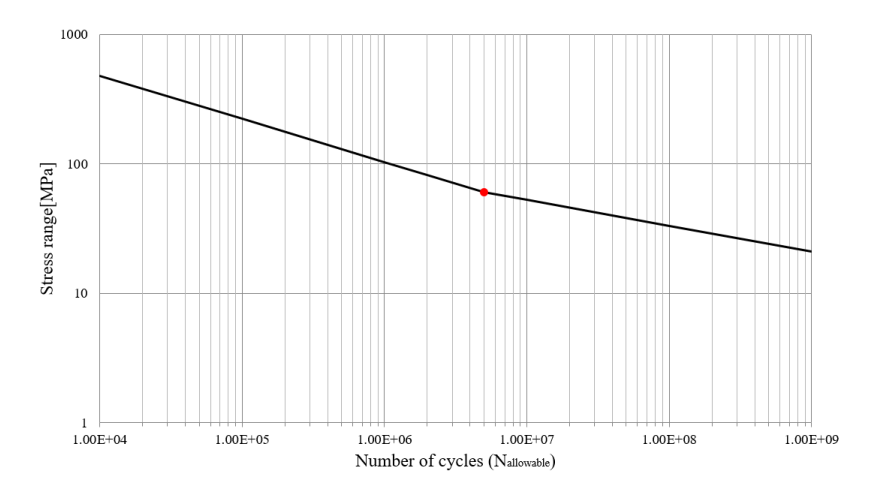


Figure 4.7: SN curve for optimized design

The results of the fatigue analysis are presented in Table 4.9. Here, $\sigma_{\rm bolt\ max}$ is the maximum expected stress during the loading of the blade root. It occurs at a bending moment of 10.5MNm. This stress is not related to the maximum and minimum moments referred to in the previous section.

	Reference	Optimized
$\sigma_{ m bolt\ max}$	637MPa	744MPa
Bolt size	M28	M32
Prestress	540MPa	640MPa
Detail	85	83.3
k_s	1	.984
Fatigue damage	0.3493	0.2713

Table 4.9: Fatigue analysis results

4.7.2 Verification of design recommendations

The design recommendations are verified by submitting the modified APDL code to the design team of Suzlon. The design engineer analyses the model by applying the loads and extracts the stresses in the bolt and post processes it. The post processed data is then received as an excel file with the stresses, loads, and the stress ratios at the loads. This is then compared to the values extracted from the Sectional model of the Optimized design.

The stress ratio in the Sectional model is lower compared to the stress ratio in the Half model. This translates to lower stresses in the Sectional model. The stress ratio extracted from the Half model at Suzlon with design recommendations and the same is extracted from the Optimized Sectional model are contrasted in Figure 4.8.

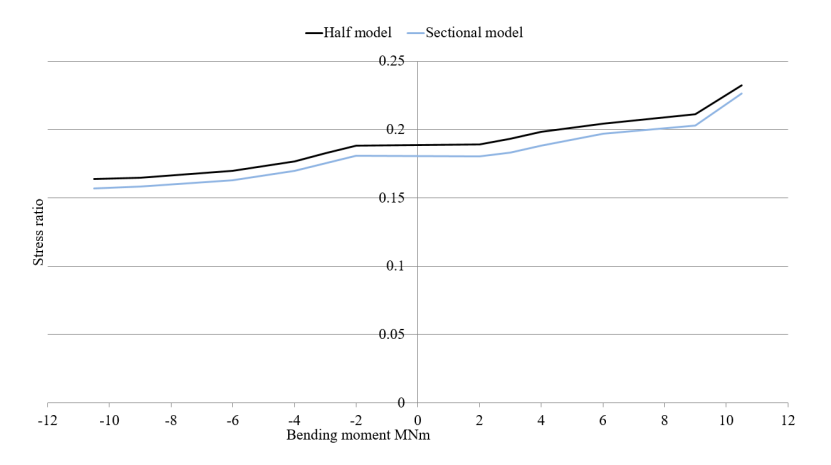


Figure 4.8: Stress ratio comparison - Half model vs Sectional model

Boundary conditions usually play a significant role in determining the flexibility of the system. The Half model deviates from the real blade root test specimen because of the boundary condition at the bearing. the bearing is not connected to a rigid hub. The hub, which is made of metal also deforms under load and modeling a rigid hub can result in the simulation of different stresses as compared to the test specimen. This, however, was the scope of the internship that preceded the thesis phase and the thesis itself does not try to solve this particular issue.

During the thesis, the Half model was converted to the Sectional model that used symmetry boundary condition on the planes that lie midway between the modeled section and its adjacent sections. Such a boundary condition could be a reason for the system being stiffer than it really is. This higher stiffness translated to larger reaction stresses at the boundaries causing lower internal stresses. When the design is translated to the Half model, the stiffness is partially alleviated at the symmetry planes, and this caused the Stress ratio to increase slightly. But, the difference between the stress ratio between Half model and Sectional model is roughly constant across the load range. This shows that the influence the design modifications have on the Sectional model is similar to the Half model. The optimized design in both the Half model and Sectional model shows a small degree of the joint opening towards the extreme loads on the tensile side. This is expected in an optimized design.

50 Optimization

Results and conclusions

In this chapter, the results of the optimization procedure are reflected upon, and a few design recommendations for the blade root are presented. The design modifications influence more than just the cost of the blade root. Factors like manufacturing times and labor time are also affected by the redesign and critically examining them will help judge the quality of the Optimized design.

5.1 Design recommendations

From the process of iterative optimization and the supporting structural analysis both prior to and after the optimization, it can be concluded that the structure of the blade root stands to benefit greatly from optimization. The design at Suzlon emphasizes structural reliability, and cost optimization was not the prime focus of the design process. Curiosity and subsequent investigation into the cost optimization of the joint revealed that on modifying key features of the joint the cost and mass could both be reduced. These design recommendations are quantified in the previous chapter and are specific to the reference design provided for the thesis by Suzlon. They are qualitatively discussed in the following sub-sections.

5.1.1 Prestress in the bolts

All mechanically fastened joints need the clamping force to keep the joints together and to manifest this clamping force, the material must be present that can be pre-stressed. To make the joint lighter the prestress in the material is increased and subsequently, the material mass is reduced. The need to increase the prestress in the T-bolt and the amount by which the prestress must be increased is to be analyzed for each design separately, and it is not proposed as a final global value. A blade root connection with higher prestress in the bolts and lower number of bolts and a few other geometry modifications shows a lower increase in the stress when in service so for the same fatigue performance it is possible to have a blade root with

lower mass. Essentially this was the initial hypothesis that founded the conceptual premise of the thesis.

The increase in the prestress of the bolts is helpful in reducing the extent of joint opening and helps it behave much more linearly. The critical load above which the nonlinear behavior comes into play is now above the maximum expected load on the blade root. Thus the required preload on the future designs must be decided depending on the expected loads and the available design. The increase in the prestress influences the bearing stress directly and to mitigate this the bearing area must be increased by widening the barrel head diameter commensurately.

5.1.2 T-bolt and blade root dimensions

After optimization, the T-bolts are roughly 45% heavier than the T-bolts in the Reference design. The T-bolt shank and barrel heads have a higher diameter. The optimization leads to a reduction in the blade root thickness and reduction in the number of bolts. This increases the bearing stress and the load per bolt. To prevent bearing failure, the bearing area is increased by increasing the barrel head diameter.

The barrel head length is constrained to be 5mm lesser than the blade root thickness. Thus, it is not a parameter available to be independently varied during the optimization. The offset of 5mm is recommended to account for the uncertainty of the thickness of the blade root. A curved structure made from Glass Fiber Reinforced Plastic (GFRP) layup provides limited precision for controlling the thickness. This gives rise to a certain degree of uncertainty in the root thickness. The real structure can show variation from the theoretical design. If the barrel head is too short, then only a portion of the laminate will be loaded in compression and the adjacent area will not be loaded increasing the risk of mode-II crack propagation between the laminate plies. This is not quantified but is a conceivable risk of improper design.

The optimizer essentially tries to reduce the overall volume of the blade root while ensuring the constraint stresses are below their design limits. During this process, the blade root thickness and the length of the transition part were found to be helpful in manipulating the mass of the blade root. This combined with the fact that the net section and shear stresses in the laminate were well below the limits, allowed the blade root to be made 10mm thinner than what it was. Owing to the large diameter of the blade root, the mass reduction in the root is sizable. The optimizer also shortened the length of the thickness transition part of the blade root and lengthened the thick part. These changes do not significantly alter the behavior of the blade root, and thus, are perceived to be safe but help in reducing the mass and cost.

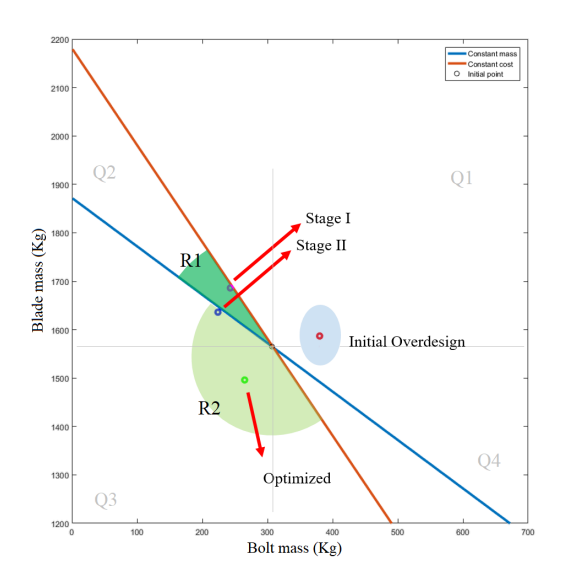
5.2 Implications of the design recommendation

In this section, the various implications of design recommendations are presented. The design proposals have an influence on more than just the material cost. It also affects the labor time and machining time required and also the influences the risk of crack nucleation in the laminate which is not quantified in the analysis but plays a sizable role in the lifetime and maintenance of the wind turbine blade root. These rather obscure aspects of the redesign will be discussed.

5.2.1 Cost implications

The blade root cost is constituted of the cost of the blade and the bolts that utilize vastly different materials. The blade is a vacuum infused GFRP layup, and the bolts are machined out of metal blocks or billets. In reality, the cost of both the components is constituted by a number of contributors including the costs of material procurement, labor cost, machine time cost, etc. Including these costs into the optimizer increases the nonlinearity of the black box function that is the cost of the blade root. Thus the decision was made to include only the material cost.

The relation between the cost and mass of the blade root is visually presented in Figure 5.1. Every possible design of the blade root can be represented as a point on the plot. This particular plot is constructed around the Reference design of the blade root.



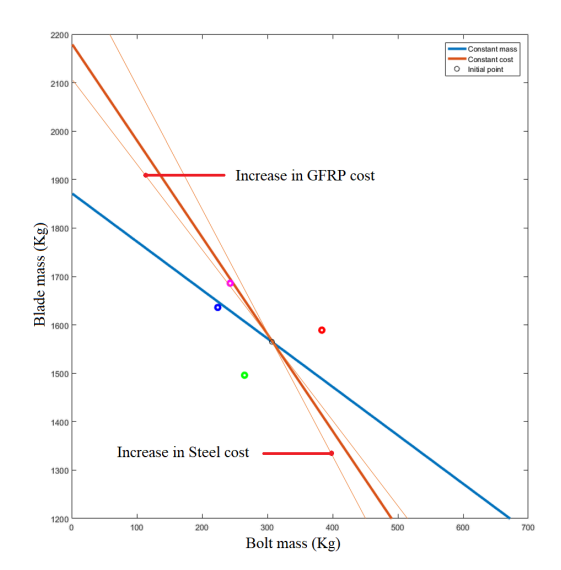


Figure 5.1: Cost-mass relation

Figure 5.2: Influence of material rates

Reference		Optimized		
	Mass (Kg)	Cost (Euros)	Mass (Kg)	Cost (Euros)
Bolts	308	1847	265	1593
Blade	1565	4696	1497	4490
Total	1875	6543	1762	6083

Table 5.1: Reference design - cost and mass

The plot is constituted of two lines intersecting at a point. The constant mass line represents all the possible designs that have the same mass as the Reference design, and the constant cost line represents all designs with the same cost as the Reference design. The intersection of the constant cost line and the constant mass line is the point representing the Reference design. The region marked R1 is the region of lower cost but higher mass. Preferably this region is to be avoided. Any design represented by a point above the constant mass line is heavier. The R1 region is also highly sensitive to the relative cost of the material in the blade root. A change in the material costs in the future will rotate the constant cost line

as shown in Figure 5.2 and this could potentially cause constant cost line to pass under the point representing the Stage I design. This makes Stage I design costlier than the Reference design if judged with the new material costs. Stage II design shows improvement in both cost and mass and can be trusted to a much higher degree than Stage I design. But, both these designs lie in the Q2 region where the designs are still susceptible to the risk of variation in material cost.

The most trusted designs can be expected to lie in the Q3 region where irrespective of the variation in the material costs the total cost will only reduce. This is because every design in the Q3 region will show a reduction in both blade mass and bolt mass. The optimized design lies in the Q3 region and thus shows great promise in the overall cost reduction.

Cost and mass saving

Since the actual cost of the blade root is not a linear function of the volume of the blade root components, the actual saving of the cost will be obscure. It is not directly quantifiable by the material cost alone. Thus as an attempt at the abstraction of the cost a parameter called the *Representative fraction* was introduced in Section 4.5.

As presented in Table 4.5 and Table 4.6, a 7% reduction in the model cost is observed. But it is important to note that the thinner part of the blade root was not a candidate in the optimization process and was modeled to realistically introduce the load into the blade root. Thus the modification of the blade root is localized in the thick blade root region as shown in Figure 5.3. The thin part of the blade root is entirely made of composite and has a mass of 1055.4Kg and a cost of 3166 Euros. This mass is not participating in the optimization process, and the cost equivalent of this must be removed from the total cost before calculating the cost advantage of the optimized design.

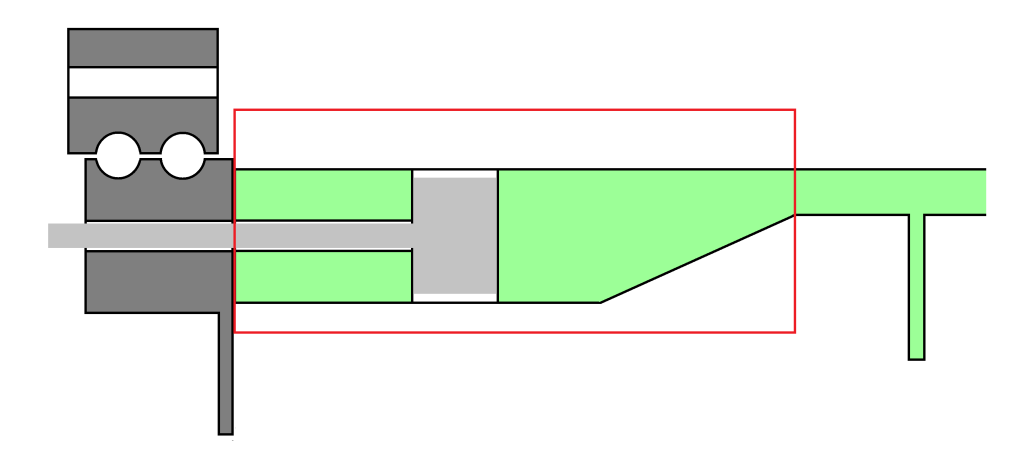


Figure 5.3: Region of modification

Thus the region being optimized represents an initial cost of 6543-3166=3177 Euros. Thus a cost saving of 460 euros represents roughly 13% of cost reduction. The absolute cost of

the blade root and its components presented in Table 4.5 and Table 4.6 are not treated as the actual cost of the respective components. This is because the rate used is the standard market rate. The real rate will vary depending on a number of factors like the source of the components and the contemporary market rates. Thus they are only representative values used to model the blade root and examine the advantage a design provides over another.

The mass, however, provides a much more clear picture of the advantage of the Optimized blade root design. The Optimized blade root is roughly 110Kg lighter than the Reference design, and this advantage can be expected irrespective of external factors because the density of the material and its volume is typical for a model and well defined in the FEM model.

5.2.2 Manufacturing implications

The design recommendation for the blade root does not radically redesign the blade root thus the fundamental manufacturing processes are the same. The optimized design has a thinner root with a lesser number of bolt holes drilled in the laminate. This translates to a lower number of plies used in the layup and lesser preparation time, machining time and labor cost. The machining time spent in creating the holes for the T-bolts is dwarfed by the time required to manufacture the root laminate. Thus, an improvement in net production time is not expected. The optimized design has a thinner blade root. This can potentially result in improved rate of vacuum infusion and better thermal characteristics during curing. The curing rate is dependent on the resin properties and is not affected.

The manufacturing of the T-bolt is by a third party that accepts drawings of the T-bolts as the input. Thus it is expected that this manufacturer has other clients. Thus, a change in the T-bolt barrel head dimensions will require using a different size billet or block of metal for machining. The bolt shank has threads on either end with a pitch diameter of 39mm which is unchanged in the optimized design. The bolt shank is smooth and has a diameter of 32mm, and thus the billet or block used for the T-bolt shank will not need changing. The machining time, however, will be lower as the mass removal will be reduced. The final rate of the T-bolt will not be vastly different from the reference rates. And even in the event of a sizable change in rates, the Optimized design is still expected to be the cheaper option compared to the Reference design.

Compared to the Reference design which has 88 T-bolts embedded in the laminate the Optimized design has only 52 such bolts. The size and length of the in-plane holes for the T-bolt shank are unchanged, and the barrel head hole drilled perpendicular to the laminate has a higher diameter. Since the total mass of the bolt has reduced, so has the volume of the laminate to be drilled out. Assuming constant mass removal rate in the shop-floor the time spent in drilling and finishing the holes is expected to reduce.

5.2.3 Fatigue life and maintenance implication

The confidence in the prediction of fatigue life of a structure reduces if the probability of crack nucleation increases. This results in larger safety factors and subsequent over design. Thus reducing this risk of crack nucleation can be vital to structures exposed to fatigue loading. Particularly in composite materials, exposed laminate edges, ply drops and drilled holes are

potential sites of crack nucleation. Reducing these features in the structure can result in leaner structures with better fatigue life. This is however not a one step process, and multiple iterations of design and testing will be necessary for such an improvement.

The optimized design of the blade root connection has a thinner blade root section with a lesser number of bolts. This translates to a lower number of holes drilled into the laminates and a lesser number of ply drops. Both of these have positive effects on the life of the blade root laminate. This is studied qualitatively as a reduction in risk of failure.

During the maintenance of the blade root, it is positioned pointing vertically downwards, and the personnel descends into the blade root by standing on the blade root stiffener. The position of the stiffener is 60cm below the bearing-laminate interface and assists the inspection and tightening of the T-bolts. Reduction in the number of T-bolts makes the job of inspection and maintenance quicker and easier.

The fatigue model of Suzlon does not take into account increase in the stress ratio of the Blade root connection as a result of the joint opening because in the blade roots being designed at Suzlon, the local bending is not yet critical. The process of cost optimization leads to leaner designs with lesser material to combat this bending. Thus cost optimized blade root connection has a higher prestress in the bolt shank that has a larger diameter. This implies a much larger force is now required to cause similar levels of joint opening. A bolted joint subjected to both axial and bending moments show a much more substantial degree of joint opening as compared to a bolted joint loaded purely in tension. Thus the blade root connection must be designed taking into consideration the fact that the presence of the bearing exerts a considerable bending moment on the joint.

5.2.4 Effects on bearings

With the reduction of the number of T-bolts the distance between two adjacent T-bolts increases. This will cause a change in the stress state and deformations in the bearings. Investigating into the implications of these secondary effects may be necessary for the future. The study of the bearing deformation is out of the scope of the thesis and is not carried out.

The bearings are manufactured at a stage subsequent to the design of the blade root. Thus the design of the bearings is customized for the contemporary design. The design changes in the blade root cause a few features in the bearing to be modified. Reduction in the number of bolts and change in pitch radius of the T-bolt will require an appropriate adjustment in the holes drilled into the bearing. The design modification doesn't require a radical redesign of the bearing, and since Suzlon has been though numerous designs of the blade root each with increasing number of bolts, the manufacturer should be able to adapt to the changes quickly.

5.3 Conclusions

The project has a positive outcome, and the process of optimization was successful. The initial hypothesis was proved to be true, and a possibility for a cheaper and lighter blade root connection was realized. It was also possible to draw up a set of design recommendations that will help optimize future designs and to aid the process of optimization an abstraction or

5.3 Conclusions 57

way of thinking is outlined so that any design can be prepared for optimization. To conclude the thesis the proposed central questions and sub-questions can now be answered. At first, the first set of sub questions will be answered, and subsequently, their corresponding central question will be addressed followed by the next set in the same order.

What is a suitable performance parameter that can be used to study the joint?

The most suitable parameter for analyzing the performance of the blade root is the **Stress ratio** of the joint. This is also the parameter that the engineers at Suzlon are familiar with as they use it for studying the blade root. The stress ratio of a joint can clearly show the joint opening and can be a useful indicator for when the joint is not performing as required.

What are the design parameters in the blade root that can be used to manipulate the performance of the joint?

The stress ratio of the joint has to be manipulated only if there is joint opening that effects the joint performance throughout the load range. This joint opening appears as a sharp increase in the stress ratio curve. A sharp increase in the stress ratio indicates the clamping force has been overcome by the combination of local bending and external loading. Thus the intent is to increase the clamping force, which is a function of the bolt area, and the prestress in the bolt. But, it was found favorable to improve the performance of the joint without increasing the mass. This is done by increasing the prestress of the bolt as increasing the bolt radius will make the bolt heavier.

Apart from the performance parameter of the joint, its reliability is indicated by the constraint stresses. These stresses can be effectively modified by manipulating the areas associated with these stresses. Thus increasing the blade root laminate thickness and the diameter of the barrel head and bolt shank can help reduce the constraint stresses and improve the reliability of the joint. This is done during the initial over design stage of the optimization phase.

What are the design parameters in the blade root that can be used to manipulate its mass?

The best parameters that can modify the mass of the blade root are the parameters that define the cross-section of the blade root. They are listed below for convenience.

- 1. The blade root inner radius (Ri)
- 2. The length of the thick part of the blade root (L1)
- 3. The length of the transition part of the blade root (L2)
- 4. The number of bolts in the blade root (Nb)

The dimensions of the bolt are direct manipulators for the constraint function and are chosen to be manipulated manually. The number of bolts, however, has an immediate impact on the mass of the joint and is chosen to be an optimization parameter. The number of parameters is kept as low as possible to ensure fast convergence. A nonlinear black box problem will benefit from having a limited number of parameters. Having a large number of parameters may also cause failure while modeling the blade root if the set of parameters calculated is not physically constructible. This may require complex or dynamic boundary functions which are not currently supported by SciPy or Matlab.

Q1: What parameters can be used to prepare the blade root design for optimization and subsequent setting up of the optimizer?

The inner radius of the blade root (Ri), the length of the thick part (L1), the length of the thickness transition region (L2), and the number of bolts (Nb) are the parameters chosen to be input parameters during the optimization phase. The dimensions of the T-bolt are the parameters (Barrel head diameter (Bhd) and Bolt shank radius (Bd)) that can be used to manipulate the constraint stresses. This is not an exhaustive list by any means, but for this particular blade root design, the above mention parameters act as reliable manipulators to modify the blade root design. For future designs, additional parameters may be used, but their selection must be made based on the blade root design and its study.

Now the second set of sub questions and subsequently the second central question is answered.

What is an appropriate definition for the degree of optimization and simplification?

Unlike the aerospace industry, where performance and reliability outweigh the cost of the structure, in the Renewable Energy industry, cost plays a major role. Often the number of blades manufactured can be measured in thousands, and the manufacturing process is often labor intensive due to the nature of raw materials and manufacturing processes involved. Thus, minimizing the cost is a very prudent venture. Reducing the number of bolts influence not only the cost but also the risk of failures and ease of maintenance.

Every hole drilled in a laminate and every extra bit of exposed laminate edge is a potential crack nucleation site. Reducing features like this can positively impact the reliability of the blade root connection and the manufacturability of the structure. Lowering the number of bolts also makes assembly less tedious and time-consuming. Thus, while searching for an optimized design, the aim is to reduce the mass and cost of the blade root, while treating the reduction in the number of bolts as a desirable but non-mandatory outcome.

What are the design constraints for the blade root?

The design constraints are identified independently from the literature survey and are also provided as an input by the engineers at Suzlon. These are the stresses in the blade root. The net-section, bearing, shearing, and bolt stresses must be below the design limits that are provided by Suzlon. The constraints on the bolt stress are two fold. The stress at the damage equivalent load in the modified design must be strictly lower than the corresponding stress in the reference design. This is a highly approximate method of ensuring the optimized design doesn't badly fail in the fatigue analysis phase later in the optimization procedure. Such a failure may invalidate the time-intensive process of the cost optimization. The bolt must also not fail at the extreme loading condition.

The other constraints are thumb rules to ensure reliable design. They apply to the design parameters in the Ansys Parametric Design Language (APDL) code and are not functions in the Python script. These restrictions include the length of the barrel head the thickness of the root and the diameter of the bolt shank. The barrel head must not project out of the laminate and must lie in the center to avoid Model II crack propagation. It is not desirable for the thickness of the blade root to be so high that the blade root overlaps with the bearing stiffener. The diameter of the bolt shank must not exceed the diameter of the hole drilled in the laminate and bearing. If the need arises, the laminate and bearing hole diameter must

5.3 Conclusions 59

be modified. In the future, depending on the design and the optimization requirements, the design constraints may vary, and the above-mentioned thumb rules are limited to the design in focus. The upper and lower bounds for the design parameters are decided arbitrarily but ensure that the dimensions of the blade root don't disrespect the design thumb rules.

What algorithm can be used to search for the optimized design?

There are a variety of optimizer algorithms available in the SciPy package, used for the scientific application of Python. The most attractive algorithms are the ones that allow for constrained optimization at the fastest rate. Four of the most robust and well-developed algorithms were reviewed and were tested purely on the basis of the rate of optimizing a smooth and well behaved mathematical function. The fastest of the four, by a considerable margin, is the Sequential Large Scale Quadratic Programming (SLSQP) algorithm. SLSQP is also the algorithm used by the engineers at Suzlon for their optimization needs. In the online forums like stack exchange, SLSQP is usually recommended to replace other algorithms when they fail to optimize their function. This significantly boosted the confidence in the algorithm. SLSQP may also be called the Sequential Quadratic Programming (SQP) algorithms based on the software being used.

Does the recommended changes for the optimization of the blade root have the same effects on the performance of Suzlon's Half model of the blade root?

The verification of the design recommendations was successful, and the Half model of Suzlon behaved very similarly to the Sectional model used for the optimization of the blade root design. This is studied by extracting the Stress ratio of the two models and contrasting them. But there were differences due to the boundary conditions used. The stress ratio extracted from the Sectional model was compared with the stress ratio of the Half model. The Half model shows 3-5% higher stresses than the Sectional model. This is predicted to be due to the stiffening nature of the symmetry boundary conditions.

The recommended changes to the blade root design have the same influence on the cost of the blade root and show similar mass and cost saving in both, the Half model and the Sectional model. The stresses are within the limit of failure, and the model also passes the fatigue calculations.

Q2: What are the changes to be made to the current blade root to reduce the effects of local laminate bending on the T-bolt and reduce the overall cost?

The local bending of the laminate is inevitable unless the joint is radically redesigned and the blade root laminate is made co-linear with the hub. The source of this local bending loads is found to be the presence of the slew bearing. The increase in stresses in the T-bolt was only observed at extreme bending moments, typically above 6MNm, on the blade root. On close observation of the deformation at the joint, it was found that the large bending loads on the blade root produced local bending that pried open the joint. This indicated to insufficient clamping forces. Thus by increasing the prestress from 540MPa to 640MPa, the joint opening was reduced.

After the initial over-design aimed at lessening the criticality of constraint stresses, an SQP optimizer loop was initiated aimed at reducing the overall cost of the blade root. It iterated over 300 designs to converge successfully after multiple interruptions for the manual redesign.

The recommended design modifications as a conclusion to the thesis are given below.

- 1. Increasing the prestress from 540MPa to 640MPa, to prevent joint opening.
- 2. Strengthening the bolts by increasing the barrel head diameter from 60mm to 80mm and the bolt shank diameter from 28mm to 32mm.
- 3. Reduction in the number of bolts from 88 to 52, owing to the now stronger bolts.
- 4. Reduction in the blade root thickness from 100mm to 90mm, owing to larger net section area due to lesser number of bolts.
- 5. Lengthening the thick part of the blade root from 217mm to 225mm. This is expected to help resist the local bending of the laminate and is also necessary to prevent the barrel hole from interfering with the transition region.
- 6. Shortening the thickness transition length or ply drop length from 285mm to 230mm. This is possible due to the reduction in the thickness of the blade root. This modification also help reduce the mass of the blade root.

References

- [1] Baulker Farm Wind Turbine Blades. Renewables first. https://www.renewablesfirst.co.uk/project-blog/baulker-farm-wind-turbine-blades. Accessed: 01-06-2017.
- [2] Slewing Ring Bearings Acorn Bearings. http://www.acornbearings.co.uk/bearings/slewing-ring-bearings. Accessed: 01-06-2017.
- [3] Víctor Martínez, Alfredo Güemes, Norbert Blanco, and Josep Costa. Three–dimensional stress analysis of the t–bolt joint.
- [4] GLAS DNV. Rotor blades for wind turbines, 2015.
- [5] British Standard. Eurocode 3-design of steel structures-, 2005.
- [6] AJE Ashworth Briggs, ZY Zhang, and HN Dhakal. T-bolt bearing strengths in composite blade applications. In 15th European Conference on Composite Materials, 2012.
- [7] B. SEUFERT and A. CREMER. T-bolt attachment of a blade root of a wind turbine, December 13 2012. WO Patent App. PCT/JP2011/006,903.
- [8] I.M. Daniel and O. Ishai. *Engineering Mechanics of Composite Materials*. Number v. 13 in Engineering mechanics of composite materials. Oxford University Press, 2006.
- [9] Composites 101 Quartus engineering,. http://www.quartus.com/resources/white-papers/composites-101/. Accessed: 01-06-2017.
- [10] Pedro Ponces Camanho and FL Matthews. Stress analysis and strength prediction of mechanically fastened joints in frp: a review. Composites Part A: Applied Science and Manufacturing, 28(6):529–547, 1997.
- [11] JM Hodgkinson, DL de Beer, and FL Matthews. The strength of bolted joints in kevlar rp. ESA SP, 243:53–61, 1986.
- [12] Richard Gordon Budynas, J Keith Nisbett, et al. Shigley's mechanical engineering design, volume 9. McGraw-Hill New York, 2008.

62 References

[13] Why Choose Cold-Formed T-Bolt Pallet Rack? - unraco. http://unarcoblog.com/why-choose-cold-formed-t-bolt-pallet-rack/. Accessed: 01-06-2017.

- [14] Bosch T-Bolt Kit ZN ST 10mm M8 x 34 valin. https://www.valinonline.com/ Products/8981021345. Accessed: 01-06-2017.
- [15] Taha Benhaddou, Clement Chirol, Alain Daidie, Jean Guillot, Pierre Stephan, and Jean-Baptiste Tuery. Pre-tensioning effect on fatigue life of bolted shear joints. *Aerospace Science and Technology*, 36:36–43, 2014.
- [16] Víctor Martínez, Alfredo Güemes, Dani Trias, and Norbert Blanco. Numerical and experimental analysis of stresses and failure in t-bolt joints. Composite structures, 93(10):2636–2645, 2011.
- [17] Systematic calculation of high duty bolted joints joints with one cylindrical bolt. Systematische Berechnung hochbeanspruchter Schraubenverbindungen Zylindrische Einschraubenverbindungen. VDI, Berlin, 2003.
- [18] Germanischer Lloyd and Germany Hamburg. Guideline for the certification of wind turbines. *July 1st*, 2010.
- [19] Eric Jones, Travis Oliphant, Pearu Peterson, et al. SciPy: Open source scientific tools for Python, 2001–. [Online; accessed <today>].
- [20] Anaconda. https://www.continuum.io/. Accessed: 01-06-2017.
- [21] Stephen J Wright and Jorge Nocedal. Numerical optimization. Springer Science, 35(67-68):7, 1999.
- [22] Michael JD Powell. A view of algorithms for optimization without derivatives. *Mathematics Today-Bulletin of the Institute of Mathematics and its Applications*, 43(5):170–174, 2007.
- [23] Walter Murray. Sequential quadratic programming methods for large-scale problems. Computational Optimization and Applications, 7(1):127–142, 1997.
- [24] Rainer Storn and Kenneth Price. Differential evolution—a simple and efficient heuristic for global optimization over continuous spaces. *Journal of global optimization*, 11(4):341—359, 1997.

Boundary condition conversion

In this chapter, the conversion of the boundary conditions for the Half model to the boundary condition for the Sectional model is presented. The method of converting the moment applied on the Half model to the equivalent force on the Sectional model is derived, and the various assumptions are also presented.

A.1 Boundary condition in Half model

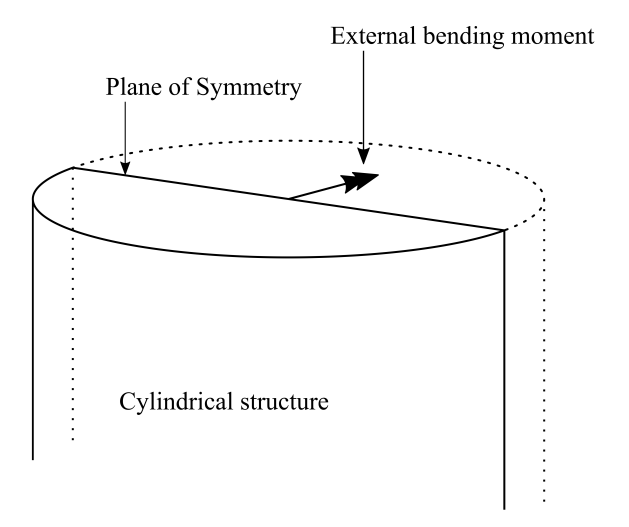


Figure A.1: Illustration of plane of symmetry in Half model

It is often recommended to exploit the planes of symmetry while setting up a Finite Element Method (FEM) model. Planes of symmetries are the planes that divide the deformation state into symmetric parts. Often there can be more than one plane. A cube subjected to hydrostatic pressure can be divided into quadrants or octants. A cylindrical structure under

tensile loading can be divided into quadrants as well. The symmetry boundary condition helps reduce the number of node, and this improves computation times.

In this particular problem, the blade root is a cylindrical structure that is subject to an external bending moment. The plane of symmetry is the axial plane perpendicular to the moment. This plane divides the cylindrical blade root into two halves as shown in Figure A.1. Adopting this simplification halves the number of nodes and improves the solution time. But it is still a large model to be solved on a consumer grade laptop.

A.2 Boundary condition in Section model

The Half model is further simplified to the Sectional model using an additional boundary plane. The boundary condition can only be applied if the interior angle of the section is sufficiently small. This is a subjective statement and must be adopted based on the accuracy needed. For the optimization process, this was seen as an appropriate method because during the verification stage the modification would finally be transferred to the Half model. It was also observed the Sectional model behaved quite close to the Half model and improvements in the two models also showed similar trends.

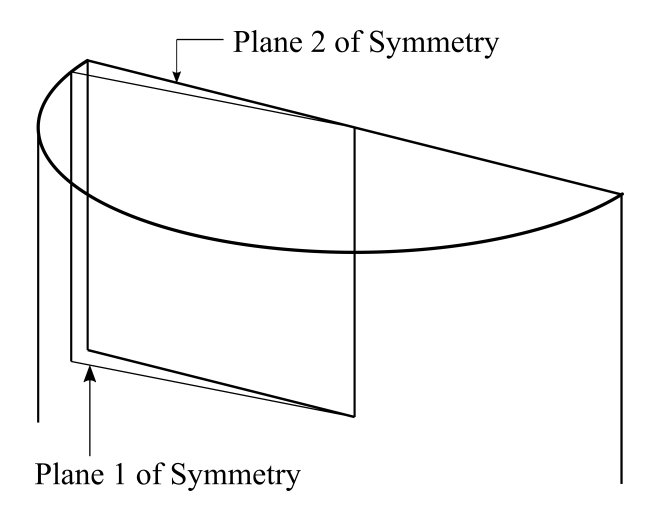


Figure A.2: Illustration of plane of symmetry in Sectional model

One of the factors that justify the Sectional model was presence of a large number of bolts. The modeled section is shown in Figure A.2. This section will experience tension due to the moment. Stresses in the cross-section of the blade root follow a sinusoidal variation as shown in Figure A.3. The modeled section lies close to the region of maximum stress. The Reference model had 88 bolts, and due to this the stresses appearing across the laminate in the modeled region was nearly uniform.

Each section is assumed to resist the external moment by providing a reaction force. The forces must also follow a sinusoidal variation as shown in Figure A.3. The i^{th} bolt provides a reaction of F_i and is placed at a distance of R_i from the axis of the external bending moment. The total external moment must be balanced by N_b such bolt forces. N_b is the number of bolts. The moment balance equation is given by Eq. (A.1).

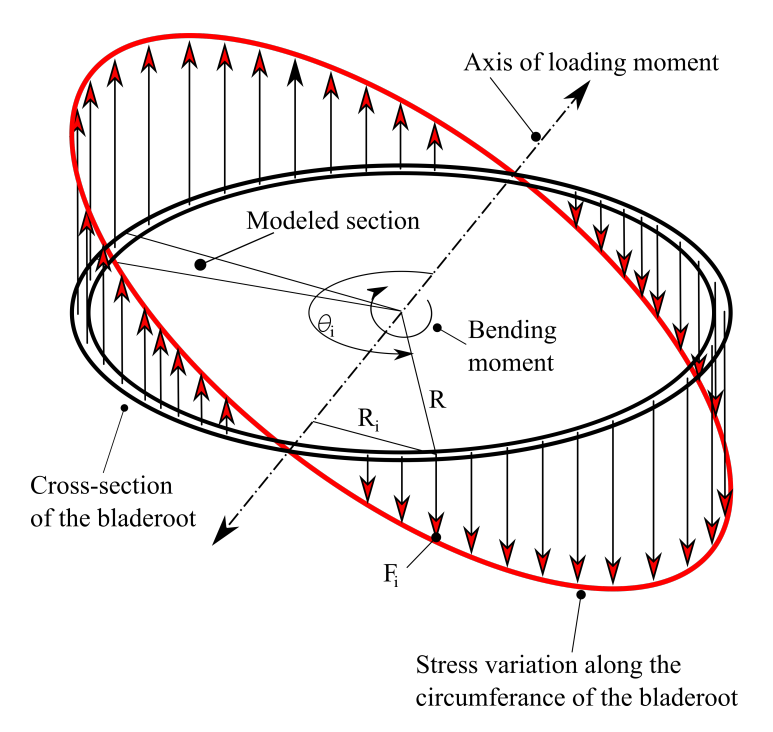


Figure A.3: Illustration of laminate stresses

$$M_{ext} = \sum_{i=1}^{N_{bolts}} M_i = \sum_{i=1}^{N_{bolts}} P_i R \sin(\theta_i)$$
(A.1)

 θ_i is the position of the i^{th} bolt along the circumference of the blade root. But P_i itself is a sinusoidal variation along θ .

$$M_{ext} = \sum_{i=1}^{N_{bolt}} P_{\max} \sin(\theta_i) R \sin(\theta_i) = \sum_{i=1}^{N_{bolts}} P_{\max} R \sin^2(\theta_i)$$
(A.2)

$$M_{ext} = P_{\text{max}} R \sum_{i=1}^{N_{bolt}} \sin^2(\theta_i)$$
(A.3)

But from theories of numerical integration one can derive,

$$\sum_{i=1}^{N_{bolt}} \sin^2(\theta_i) = \frac{N_{bolt}}{2} \tag{A.4}$$

$$\therefore M_{ext} = \frac{P_{\max}RN_b}{2} \Rightarrow P_{\max} = \left(\frac{2M_{ext}}{RN_{bolt}}\right) \Rightarrow P_i = \left(\frac{2M_{ext}}{RN_{bolt}}\right)\sin(\theta_i) \tag{A.5}$$

Since the blade root model employs a symmetric boundary condition as discussed earlier, two bolts are equally furthest from the axis of moment application. Thus, $\theta_i = 90 \pm \left(\frac{360}{2(N_{bolt})}\right)$ represents the bolt under highest load. This relation is used to convert the moment applied on the Half model to the equivalent force applied on the Sectional model.

Blade root dimensions

In this chapter, the exact dimensions of the blade root are presented, and the dimensions of the Optimized design are contrasted with the Reference design and the differences are highlighted. The various simplifications adopted to simplify the model compared to the real structure is also presented and its implications are discussed.

B.1 Dimensions of the blade root

The dimensions of the Reference blade root and the Optimized blade root are presented in Figure B.1 and Figure B.2 respectively for comparison. The modified dimensions are highlighted based on whether they have increased or reduced in magnitude. The schematic is not to scale and is for illustration only.

The blade root consists of the thick part and the transition part. When holes are drilled into a load bearing structure, it is advised to locally increase the thickness of the structure to make up for the lost load transmitting area. A reduction in the total number of holes drilled will reduce the required increase in thickness of the structure. This trend is also observed in the Optimized design. reducing the number of T-Bolts allowed the reduction of the overall blade root thickness. The initial thickness was 100mm, and this is reduced to 90mm. A 10% reduction in thickness also roughly translates to 10% lesser plies used. This will further improve the time required to prepare the plies and complexities in manufacturing, and these are highlighted in Section 5.2.

One of the important features of the transition part is the angle at with the transition of thickness happens. This can also be visualized as the rate of ply drops. This is maintained close to the reference design, and the value is presented in Figure B.2.

All other dimensions are left unmodified. The dimensions of the bearing are not manipulated as the bearing is not manufactured by Suzlon. The thinner root sits well within the limits of the bearing and does not interfere with the bearing stiffener, complying with the design thumb rules.

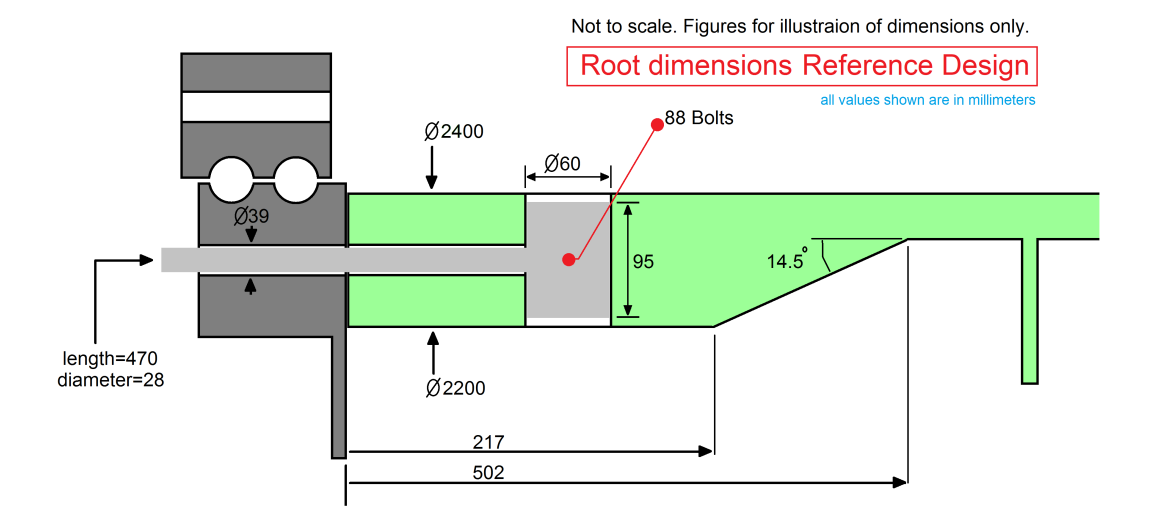


Figure B.1: Dimensions of Reference design

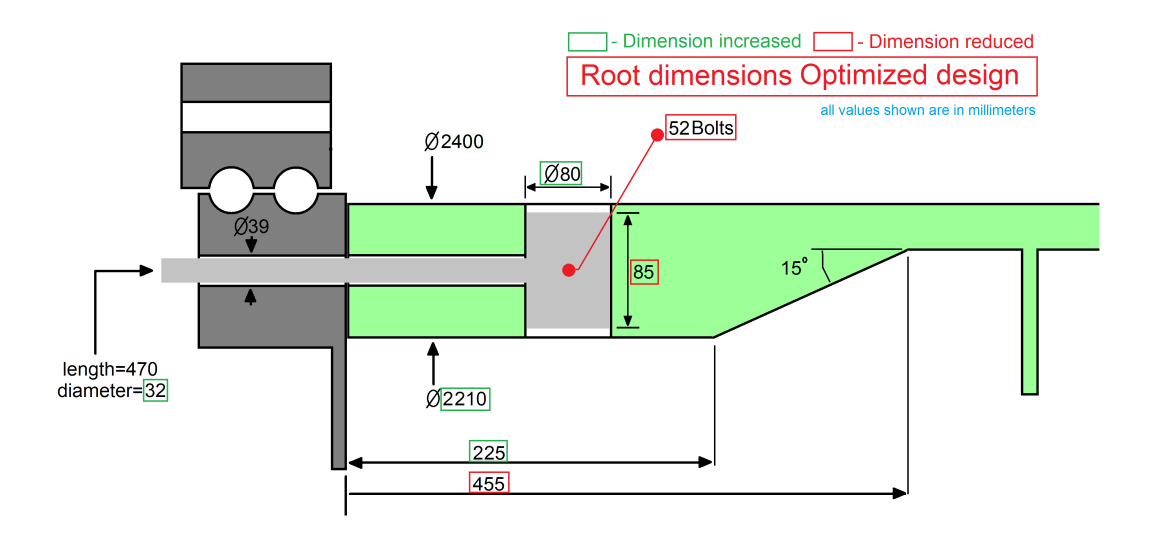


Figure B.2: Dimensions of Optimized design

B.2 Model simplification

An exhaustive illustration of the blade root dimensions are presented in Figure B.1 and Figure B.2. But they do not accurately represent the real blade root design, and a few necessary simplification have been made to the FEM model as compared to the actual test specimen. These design modifications are warranted by the fact that the FEM model is not subject to all the loads a blade root in service is subjected to. These simplifications and assumptions are presented here.

The stiffener of the blade is an important feature from the maintenance point of view. It acts as a platform on which the maintenance personnel stands to inspect the blade root joint, thereby, applying an out-of-plane force on the stiffener laminate. The real shape of the blade

root stiffener is more complicated than what is shown. It is a sandwich structure to increase the out-of-plane stiffness to prevent failure then someone stands on it. The purpose of the stiffener in the FEM design is only to provide resistance to ovalization while applying of the bending moment for which the in-plane stiffnesses of the laminate are important. The sandwich structure doesn't influence the in plane stiffnesses of the laminate. Thus this detail is ignored for simplification.

The FEM model of the blade root also does not incorporate the girders that are present in the blade root. The purpose of the FEM model is limited to studying the stress states in the joint which is assumed to be independent of the local stiffness further into the blade.